AD-A062 473 VARIAN ASSOCIATES PALO ALTO CALIF F/G 20/12
RESEARCH ON LONG WAVELENGTH BIAS-ASSISTED PHOTOEMITTER.(U)
SEP 78 J S ESCHER DAAG29-76-C-0002
UNCLASSIFIED ARO-13266.4-EL NL

| OF |
AD
A062473

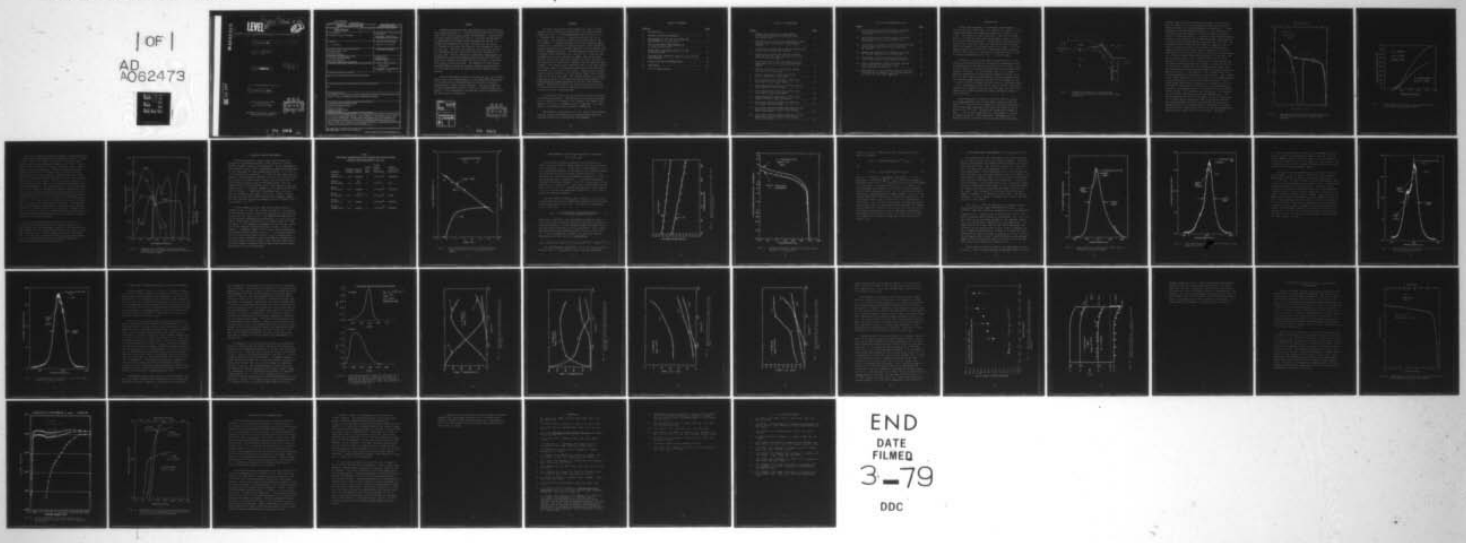

END
DATE
FILMED
3-79
DDC

(18) ARO (19) 13266.4-EL

LEVEL II

(12)

(6) RESEARCH ON LONG WAVELENGTH BIAS-ASSISTED PHOTOEMITTER.

SC

(9) FINAL REPORT. 1 Aug 75-31 Jul 78,

(10) J. S. ESCHER

(11) SEPTEMBER 1978

(12) 49p.

U. S. ARMY RESEARCH OFFICE

(15) DAAG29-76-C-0002

Varian Associates, ~~Inc.~~
611 Hansen Way
Palo Alto, CA 94303

APPROVED FOR PUBLILC RELEASE;
DISTRIBUTION UNLIMITED

UNCLASSIFIED

SECURITY CLASSIFICATION OF THIS PAGE (When Data Entered)

REPORT DOCUMENTATION PAGE

READ INSTRUCTIONS BEFORE COMPLETING FORM

1. REPORT NUMBER: ~~FINAL REPORT~~	2. GOVT ACCESSION NO.
3. RECIPIENT'S CATALOG NUMBER	
4. TITLE (and Subtitle): "Research on Long Wavelength . . . "	5. TYPE OF REPORT & PERIOD COVERED: Final Report, 1 Aug 1975 - 31 Jul 1978
6. PERFORMING ORG. REPORT NUMBER: ---	
7. AUTHOR(s): J. S. Escher	8. CONTRACT OR GRANT NUMBER(s): DAAG29-76-C-0002
9. PERFORMING ORGANIZATION NAME AND ADDRESS: Varian Associates, Inc. 611 Hansen Way Palo Alto, CA 94303	10. PROGRAM ELEMENT, PROJECT, TASK AREA & WORK UNIT NUMBERS
11. CONTROLLING OFFICE NAME AND ADDRESS: U.S. Army Research Office Post office Box 12211 Research Triangle Park, NC 27709	12. REPORT DATE: September 1978 13. NUMBER OF PAGES: 41
14. MONITORING AGENCY NAME & ADDRESS (if different from Controlling Office)	15. SECURITY CLASS. (of this report): Unclassified 15a. DECLASSIFICATION/DOWNGRADING SCHEDULE: NA

16. DISTRIBUTION STATEMENT (of this Report)

Approved for public release; distribution unlimited.

17. DISTRIBUTION STATEMENT (of the abstract entered in Block 20, if different from Report)

NA

18. SUPPLEMENTARY NOTES

The findings in this report are not to be construed as an official Department of the Army position, unless so designated by other authorized documents.

19. KEY WORDS (Continue on reverse side if necessary and identify by block number)

Transferred-electron photoemission
field-assisted photoemission
InGaAs alloys
Monte Carlo calculations
Schottky barriers

20. ABSTRACT (Continue on reverse side if necessary and identify by block number)

Transferred-electron photoemission to 1.7 microns has been achieved for the first time from a Ag/p-$In_{.53}Ga_{.47}As$ cathode. A peak reflection-mode quantum yield of 1.6% at 1.3 microns was achieved. Measurements of the optical absorption coefficient and photoluminescence spectrum of LPE-grown $In_{.53}Ga_{.47}As$/InP(100) sampes are presented. Monte Carlo calculations of the energy distributions of photogenerated electrons reaching the emitting surface are also discussed.

DD FORM 1 JAN 73 1473 EDITION OF 1 NOV 65 IS OBSOLETE

SECURITY CLASSIFICATION OF THIS PAGE (When Data Entered)

SUMMARY

Transferred-electron (TE) photoemission in the reflection and transmission-mode to 1.7 microns was achieved for the first time from a Ag/p-$In_{.53}Ga_{.47}As$/InP photocathode. A peak reflection-mode quantum yield of 1.6% at 1.3 microns was measured in an experimental ultrahigh vacuum photoemission system. Although TE photoemission has been achieved over the entire InP-InGaAsP alloy range, the focus in this program has been on $In_{.53}Ga_{.47}As$. Extensive LPE materials work has been carried out investigating the optical and electronic properties of $In_{.53}Ga_{.47}As$. Optical absorption coefficient measurements are presented along with photoluminescence and Van der Pauw data. Monte Carlo simulation studies of the TE process in p-InP and p-$In_{.53}Ga_{.47}As$ have been made. The emphasis in the calculations has been to study the electron energy distributions at the emitting surface versus applied bias and doping concentration.

Further experimental work on the Ag/p-$In_{.53}Ga_{.47}As$ cathode should focus on an understanding of the temperature dependence of the bias-assisted photoemission process and a detailed investigation of dark current emission. Electron energy distribution measurements would be helpful in understanding the physics of the photoemission process and could be compared with the Monte Carlo calculations.

FOREWORD

The work reported here was supported by the U.S. Army Research Office, Research Triangle Park, NC, under Contract DAAG29-76-C-0002. The Program Manager was initially Dr. H. R. Wittmann and, during Dr. Wittmann's absence, Dr. M. A. Littlejohn. The program is aimed at the investigation and development of a high performance III-V field-assisted photocathode and is conducted in conjunction with a more extensive program sponsored by the Defense Research Projects Agency under Contract DAAK02-74-C-0132. The ARPA program is monitored by the Night Vision Laboratory, Ft. Belvoir, VA. Since the two programs have certain features in common, most of the main results carried out under this program have been included in the quarterly and semi-annual technical reports under the ARPA program. The reader should therefore refer to the ARPA reports for further details of materials growth and vacuum activation procedures not covered in this report. Requests for the ARPA reports must be referred to the Director, Night Vision Laboratory, Ft. Belvoir, VA 22060. The present program is a continuation of an earlier field-assisted photocathode program, Contract DAHC04-73-C-0030 supported by the U.S. Army Research Office. Significant results have been published in the open literature and the reader is referred to these papers in the text and the list of publications.

The work was carried out in the Varian Corporate Research Solid State Laboratory. Contributions to this work were made by J.S. Escher, P.E. Gregory, G.A. Antypas, S.B. Hyder, Y.M. Houng, S.H. Chiao, R. Sankaran, and T.J. Maloney. S.C. Reita and H.L. Gilliland provided technical assistance.

The technical leadership of Dr. R.L. Bell of this laboratory and helpful discussions with Professor W.E. Spicer of Stanford University are gratefully acknowledged.

TABLE OF CONTENTS

LIST OF ILLUSTRATIONS

LIST OF ILLUSTRATIONS (Cont.)

1. INTRODUCTION

Present photocathodes, including the newer negative-electron-affinity (NEA) types, are limited to a useful ($\geq$ 0.1% quantum efficiency) photoemission yield out to about 1.1 microns. The reason for this limitation is due, for the most part, to a practical work function minimum of about 1.0 eV at the electron emitting surface. Externally-biased photocathodes however can extend this limit by lowering the vacuum energy level with respect to the Fermi level in the bulk. It is the general purpose of this work to investigate the transferred-electron (TE) effect in various III-V semiconductors in order to achieve photoemission into the 1 - 2 micron range.

A number of p-n junction, MOS, Schottky-barrier, field-emission, and heterojunction bias-assisted photocathodes have been proposed and experimentally studied over the years. None of these however has shown reasonably efficient photoemission beyond 1.1 microns. In 1974 however, Bell et al[1] experimentally demonstrated a bias-assisted Ag/p-InP cathode using for the first time the TE mechanism to achieve photoemission. The long wavelength threshold was that of the bandgap of InP, $\sim$ 1.35 eV, and the quantum yield with bias was reasonably good, $\sim$ 0.5%. Encouraged by this result, work at Varian on TE photocathodes has progressed steadily over the past four years with significantly higher yields and longer wavelength response being achieved.

TE photoemission is based on the fact that for certain III-V semiconductors such as InP, GaAs, InGaAsP alloys and others [2,3] electrons can be promoted to the upper conduction band valleys with reasonable efficiency for electric fields greater than 10^4 V/cm. Consider the energy band diagram of Fig. 1. The cathode shown here is a low bandgap ($\sim$ 0.9 eV) p-InGaAsP alloy on a p-InP substrate. Photogeneration of minority carrier electrons can be achieved either by photons

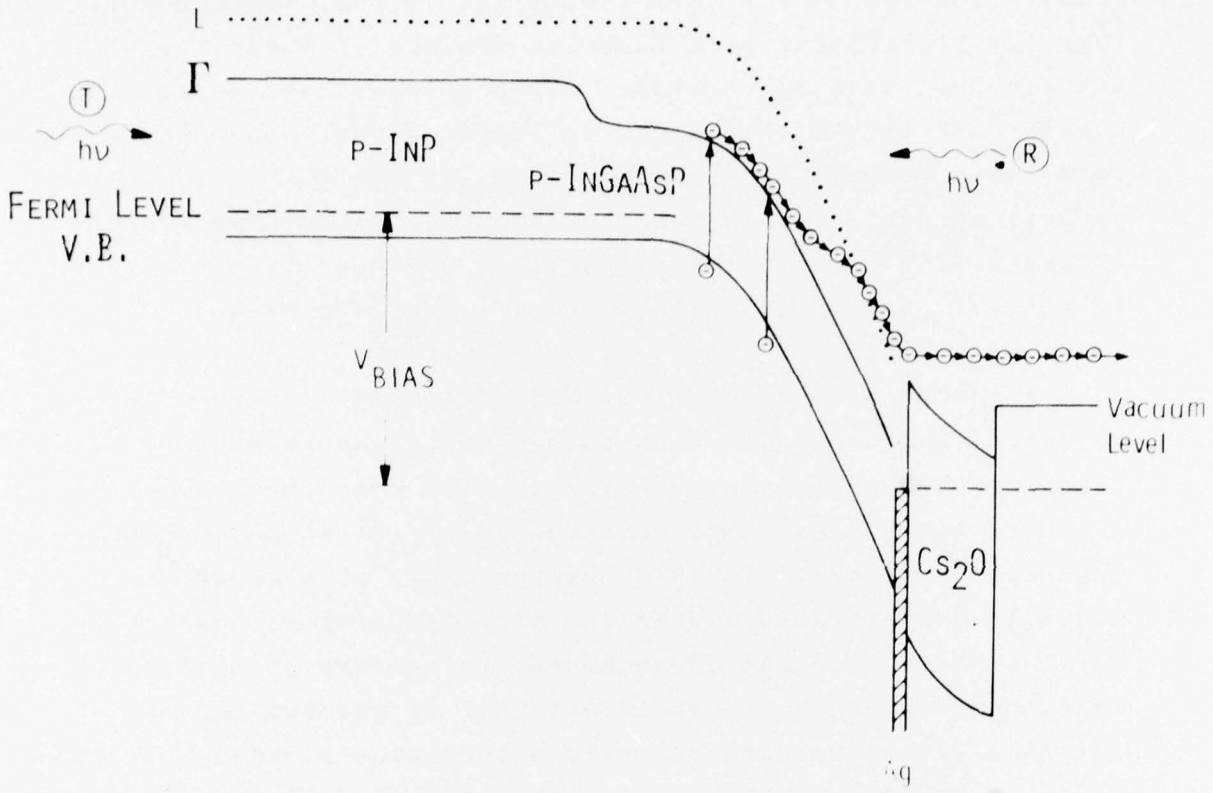

Fig. 1. Energy band diagram of a Ag/p-InGaAsP transferred-electron photocathode under bias conditions.

incident upon the electron emitting surface, the reflection-mode of operation, R, or by photons incident upon the back substrate side, the transmission-mode of operation, T. Photo-generated electrons quickly thermalize to the bottom of the Γ-conduction band minimum and a fraction begin to diffuse toward the emitting surface. A reverse biased Schottky-barrier surface contact depletes the p-InGaAsP cathode, establishing a field near the emitting surface of greater than 10^4 V/cm. The p-InGaAsP electron emitting layer must be lightly p-type in order to achieve reasonably low internal Schottky-barrier leakage currents and at least several tenths of a micron of high electric field region needed for efficient electron transfer. Electrons which successfully transfer to the upper conduction band valleys (e.g., L and X in the case of III-V alloys) or sufficiently hot Γ-electrons are then emitted over the surface energy barriers into vacuum. A low work function is attained by treatment of the Schottky-barrier metal and emitting surface with cesium and oxygen in a fashion similar to NEA activations.[4] A thin Ag film ~ 150 Å thick serves as an electron-permeable, hole-barrier biasing contact. Fig. 2 shows R and T-mode quantum yield curves from a ~ 0.9-eV Ag/p-InGaAsP cathode showing zero bias and bias-assisted yield.[5] The T-yield being higher than the R-yield is a combined result of a low surface recombination velocity at the cathode-substrate interface, a reasonably good (> 1.0 micron) electron diffusion length, proper active cathode layer thickness, 1 - 2 microns, and a polished, antireflection-coated substrate back. The short wavelength cut-off at 0.95 micron in the T-yield is due to the sharp optical absorption edge of the p-InP substrate. The long wavelength threshold is determined by the direct bandgap of the active cathode layer. The onset of the bias-assisted yield is typically 0.5 to 1.0 V and the maximum bias-assisted yield occurs for a 5 to 10 V bias. See Fig. 3.

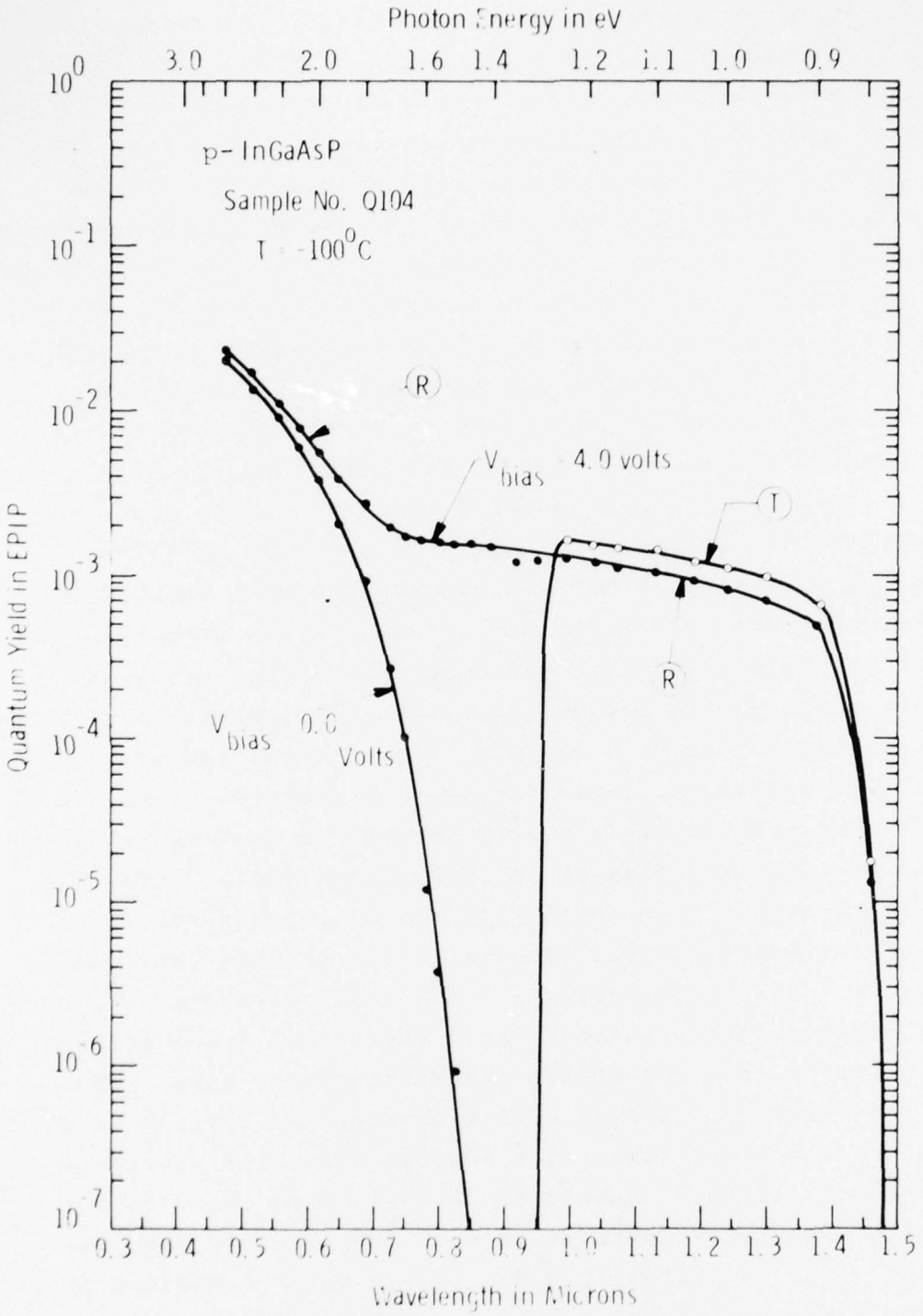

Fig. 2. Experimental reflection and transmission-mode quantum yield curves from a Ag/p-InGaAsP cathode.

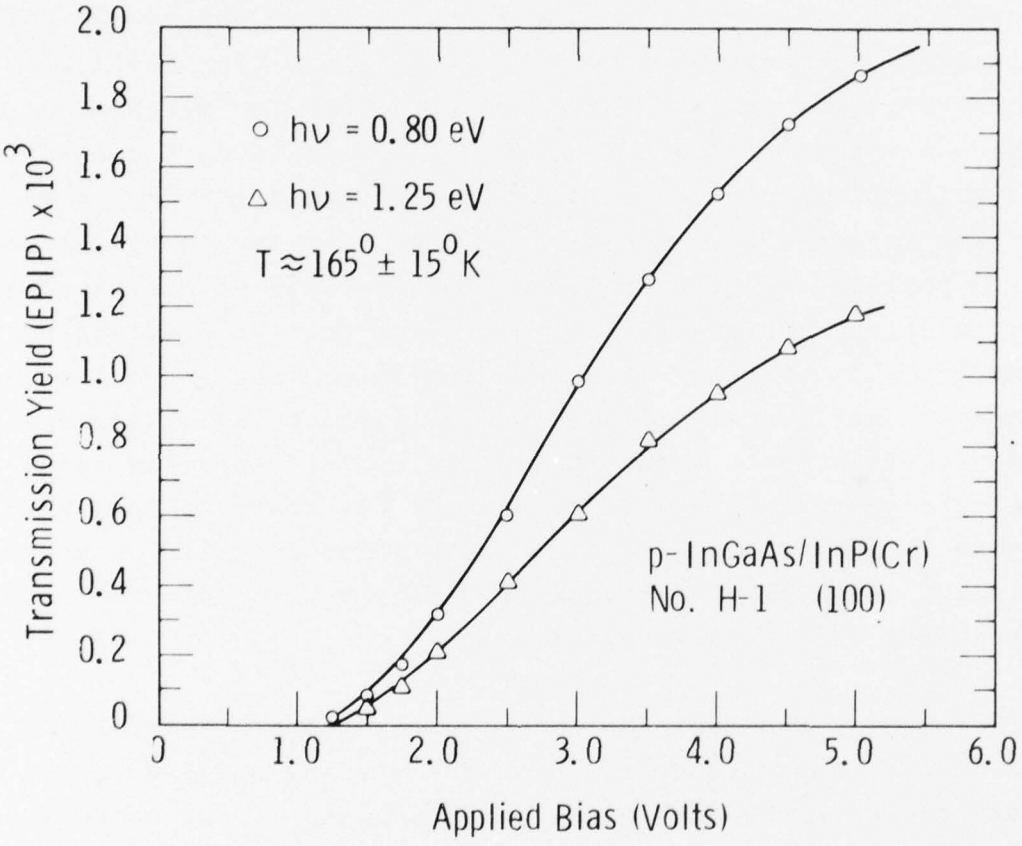

Fig. 3. Transmission quantum yield versus applied bias from a Ag/p-$In_{.53}Ga_{.47}As$ cathode.

Dark current emission from TE cathodes is characterized by a rapid increase with applied bias beginning below 10^{-12} A/cm^2 to values above 10^{-6} A/cm^2. The onset of detectable bias-assisted dark current emission is typically ~ 1.0 V. A cold cathode effect can occur if the active p-type cathode layer is grown on an n-type substrate. Reverse biasing the surface Schottky- barrier is at the same time forward biasing the substrate-epitaxial p-n junction, thereby injecting a large number of electrons from the substrate into the active cathode layer and hence into vacuum.[1] Ideally a p-type substrate, or a suitably-grown buffer layer, is necessary for meaningful dark current measurements. The rapid increase in dark current with applied bias suggests a mechanism of impact ionization by hot holes injected by the reverse-biased Schottky-barrier contact.[5] The maximum electric field near the surface of the metal-semiconductor interface is ~ 1 x 10^5 V/cm for 10^{16}/cm^3 doping and modest 3 - 5 V bias. Electric fields on this order are necessary to achieve significant impact ionization. Unfortunately detailed information on ionization coefficients for holes and electrons in InGaAsP alloys are not available. However using some early data on InP[6] and a simplified analysis shows that an impact ionization mechanism for dark current emission from TE cathodes is certainly plausible.

One of the important applications of a practical 1 - 2 micron photocathode would be for a passive night vision device where the long wavelength response of the cathode could take advantage of the strong airglow radiation beyond 1 micron. Fig. 4 shows a set of cathode response curves for NEA GaAs, S-20, S-1, and a TE cathode of Ag/p-$In_{.53}Ga_{.47}As$ under modest bias. The outstanding potential of the TE cathode for 1 - 2 micron applications is clearly evident.

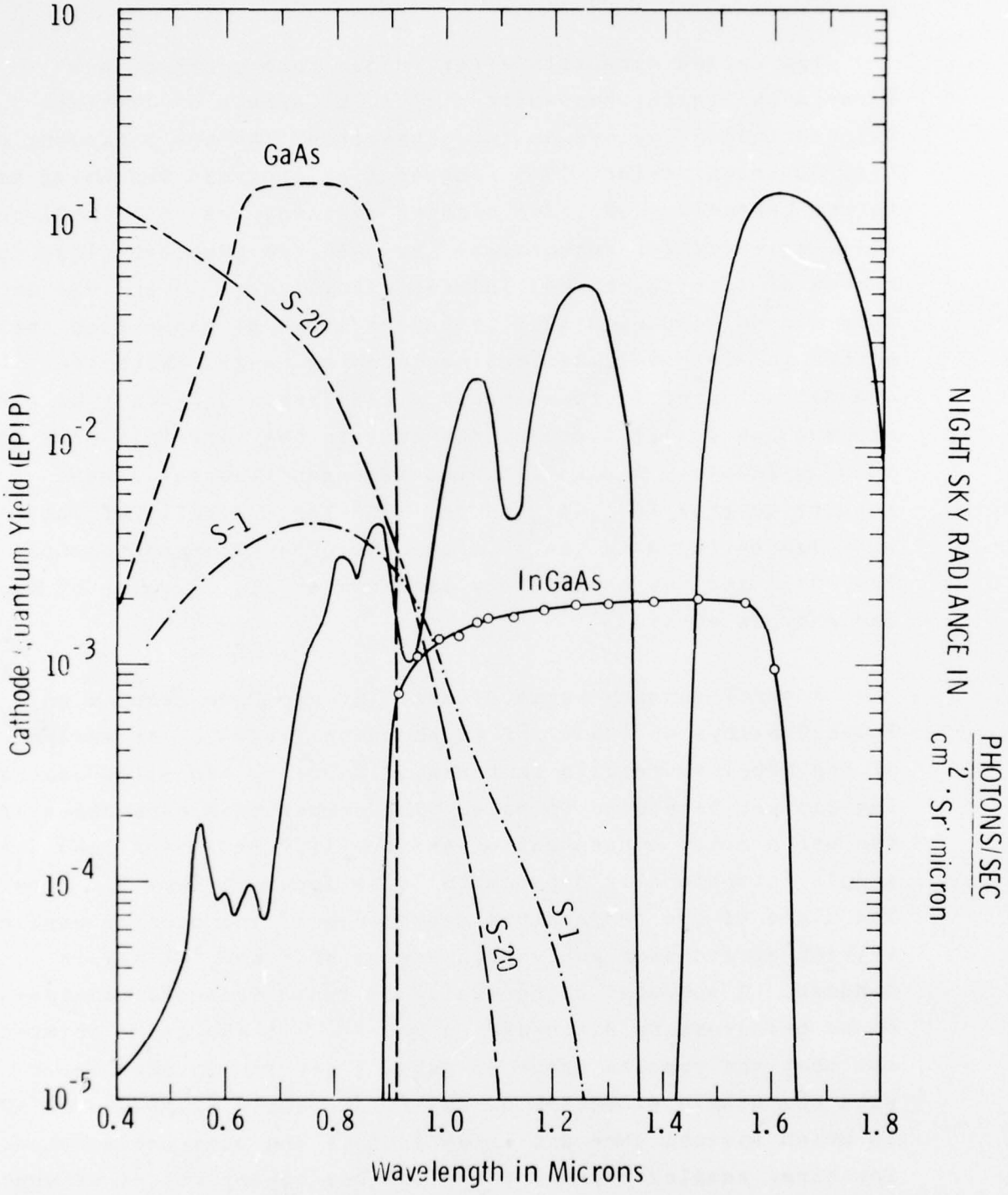

Fig. 4. Quantum yield curves for various cathodes compared with the night sky radiance in the 0.4 to 1.8 micron range.

2. MATERIALS GROWTH EXPERIMENTS

The entire materials effort under this contract has focused on liquid-phase-epitaxial (LPE) growth of lattice-matched InGaAsP alloys on InP substrates. At the beginning of this contract period, 1975, encouraging progress was being made in the LPE growth of lower bandgap quaternaries (< 1.0 eV) on (111)-oriented InP substrates. By 1976 the LPE technology for growth of lattice-matched InGaAsP alloys on (111)-InP was under good control and high quality layers could be grown over the entire InP-$In_{.53}Ga_{.47}As$ lattice-matching range. With the demonstration of field-assisted yield from a Ag/p-$In_{.53}Ga_{.47}As$ cathode out to 1.7 microns, emphasis in the materials area has been on InGaAs. A significant development was the recent ability to grow $In_{.53}Ga_{.47}As$ on (100)-InP. Details of this work can be found in the ARPA reports under Contract DAAK02-74-C-0132 and the articles by Sankaran et al,[7,8] Hyder et al,[9] and Antypas et al.[10,11]

A brief summary table of some Van der Pauw results on InGaAsP alloys on (100) InP is shown in Table I. An analysis of the mobility results in terms of impurity and alloy scattering has not been done to date. The temperature dependence of the net carrier concentration and mobility in a p-$In_{.53}Ga_{.47}As$ sample intentionally doped with Zn is shown in Fig. 5. From the slope of the temperature dependence of the carrier concentration an acceptor activation energy of 8 meV $\pm$ 2 meV is deduced. A somewhat higher value is found from photoluminescence measurements discussed in Sec. 4. It should be pointed out that the results shown in Table I are for unbaked melts with the single exception of the first sample (# FB-QF-1001-0) in which special care was taken in melt and boat preparation. The other samples represent typical day-to-day values without special melt or boat preparations.

TABLE I

ELECTRICAL PROPERTIES OF LPE InGaAsP AND InGaAs LAYERS GROWN ON SEMI-INSULATING (100) InP

Sample No.	Bandgap(eV) at 300° K	Dopant (atom %)	Conductivity Type	Carrier Density (cm^{-3}) 300° K/77° K	Mobility (cm^2/V-sec) 300° K/77° K
InGaAsP FB-QF-1001-0	1.20	Undoped	n	$8.6/3.1 \times 10^{15}$	2366/42837
InGaAsP FB-SQ-1902-0	1.20	Zn 5×10^{-5}	p	4.5×10^{15}/---	120/---
InGaAs FA-ST-2501-0	0.75	Undoped	n	$1.7/1.4 \times 10^{16}$	7573/14424
InGaAs FA-ST-2502-0	0.75	Zn 3.5×10^{-4}	p	$4.7/2.3 \times 10^{16}$	98/225
InGaAsP FA-QT-802-0	1.04	Undoped	n	$2.0/1.8 \times 10^{16}$	4094/9091
InGaAsP FB-SQF-090-23	0.95	Undoped	n	$1.8/1.7 \times 10^{16}$	4165/6553

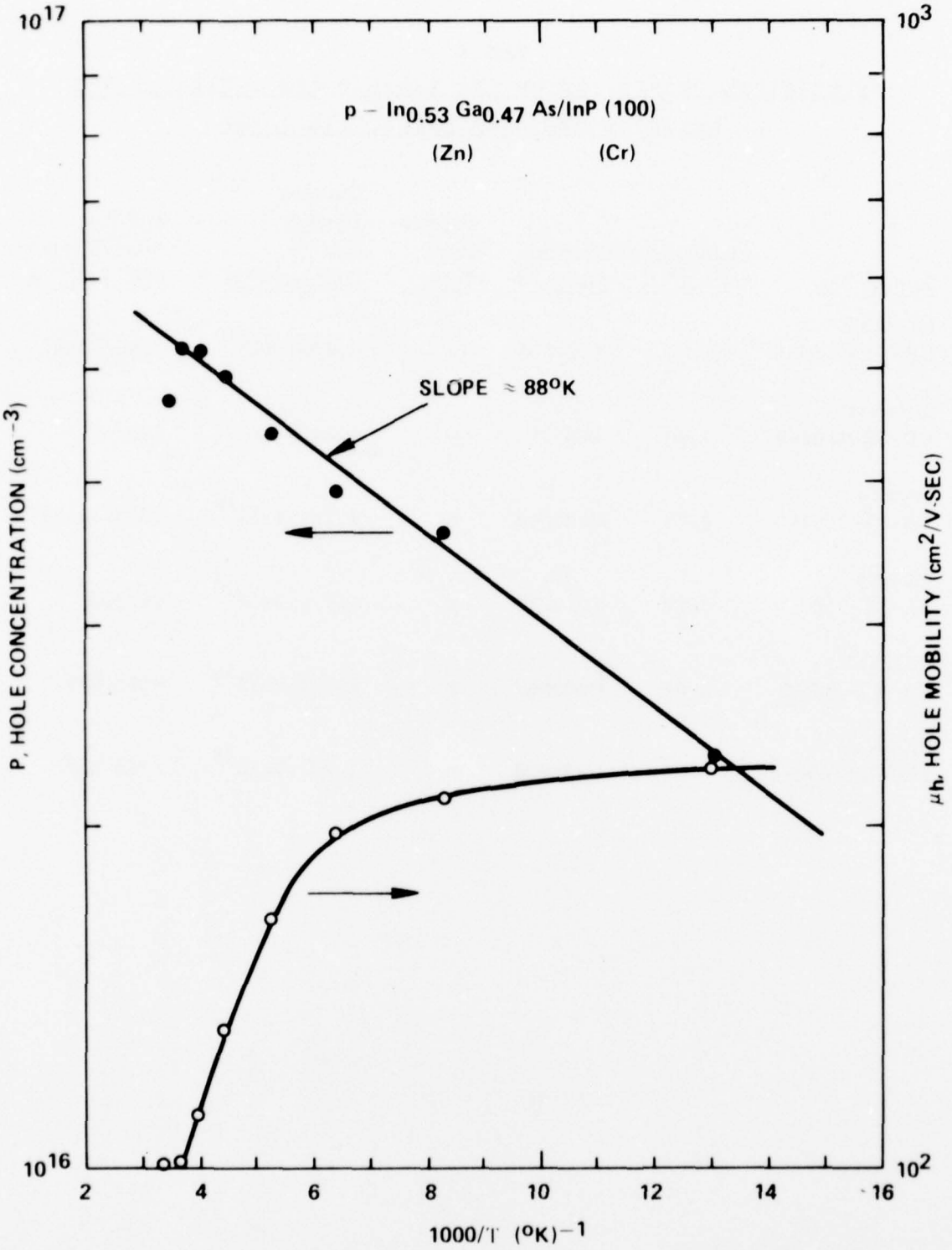

Fig. 5. Hole concentration and hole mobility versus temperature for a p-$In_{.53}Ga_{.47}As/InP(100)$ sample.

3. MEASUREMENT OF THE OPTICAL ABSORPTION COEFFICIENT OF $In_{.53}Ga_{.47}As$

An important parameter needed in the optimization of almost all optoelectronic applications is the optical absorption coefficient, $\alpha(h_\nu)$. In the case of photocathodes, $1/\alpha(h_\nu)$ is an approximate measure of the depth of photoelectron generation from the surface of incident photon radiation. It is important that the active photocathode thickness be >> than $1/\alpha$ for reflection mode cathodes and $\simeq 1/\alpha$ for semitransparent cathodes for optimal response. $\alpha(h_\nu)$ for $In_{.53}Ga_{.47}As$ has been measured by Y. Takeda et al[12] only over a narrow photon energy range of 0.75 - 0.82 eV. We have extended these measurements to 1.10 eV and give an approximate formula for α vs h_ν that is useful for modeling purposes.

The measurement technique used to measure $\alpha(h_\nu)$ was that of measuring the optical transmittance through a thin epitaxial InGaAs layer grown on InP (100). The optical transmittance $T(h_\nu)$ is given by

$$T(h_\nu) = \frac{[1 - R1(h_\nu)][1 - R2(h_\nu)]\exp(-\alpha(h_\nu)t)}{1 - R1(h_\nu)R2(h_\nu)\exp(-2\alpha(h_\nu)t)} \quad , \quad (1)$$

where $R1(h_\nu)$ and $R2(h_\nu)$ are experimentally measured optical reflectance from the InGaAs surface and the back (polished) InP substrate surface. t is the measured InGaAs epitaxial thickness which was 3.85 microns in this experiment. Fig. 6 shows the measured optical reflectance data from 1.25 to 0.75 eV. Eq. (1) can be rewritten to deduce $\alpha(h_\nu)$ directly from the experimental, R1, R2, and $T(h_\nu)$ measurements.

$$\alpha(h_\nu) = \frac{1}{t}\ln\{(1-R1)(1-R2)/2T + [(1-R1)^2(1-R2)^2/4T^2 + R1R2]^{1/2}\} \quad (2)$$

The experimentally determined α vs h_ν for $In_{.53}Ga_{.47}As$ is shown in Fig. 7. Also shown in Fig. 7 are two calculated

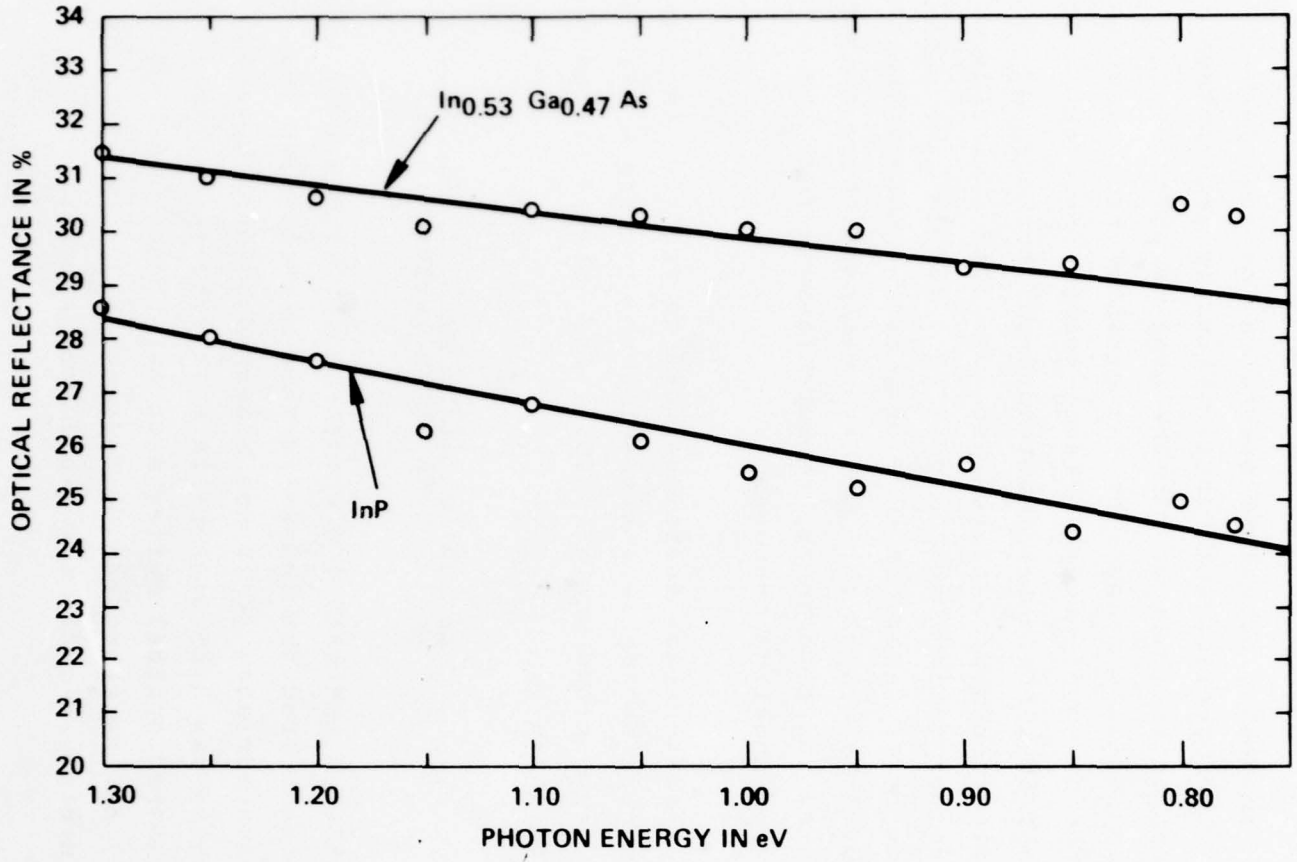

Fig. 6. Optical reflectance versus photon energy from InP and $In_{.53}Ga_{.47}As$.

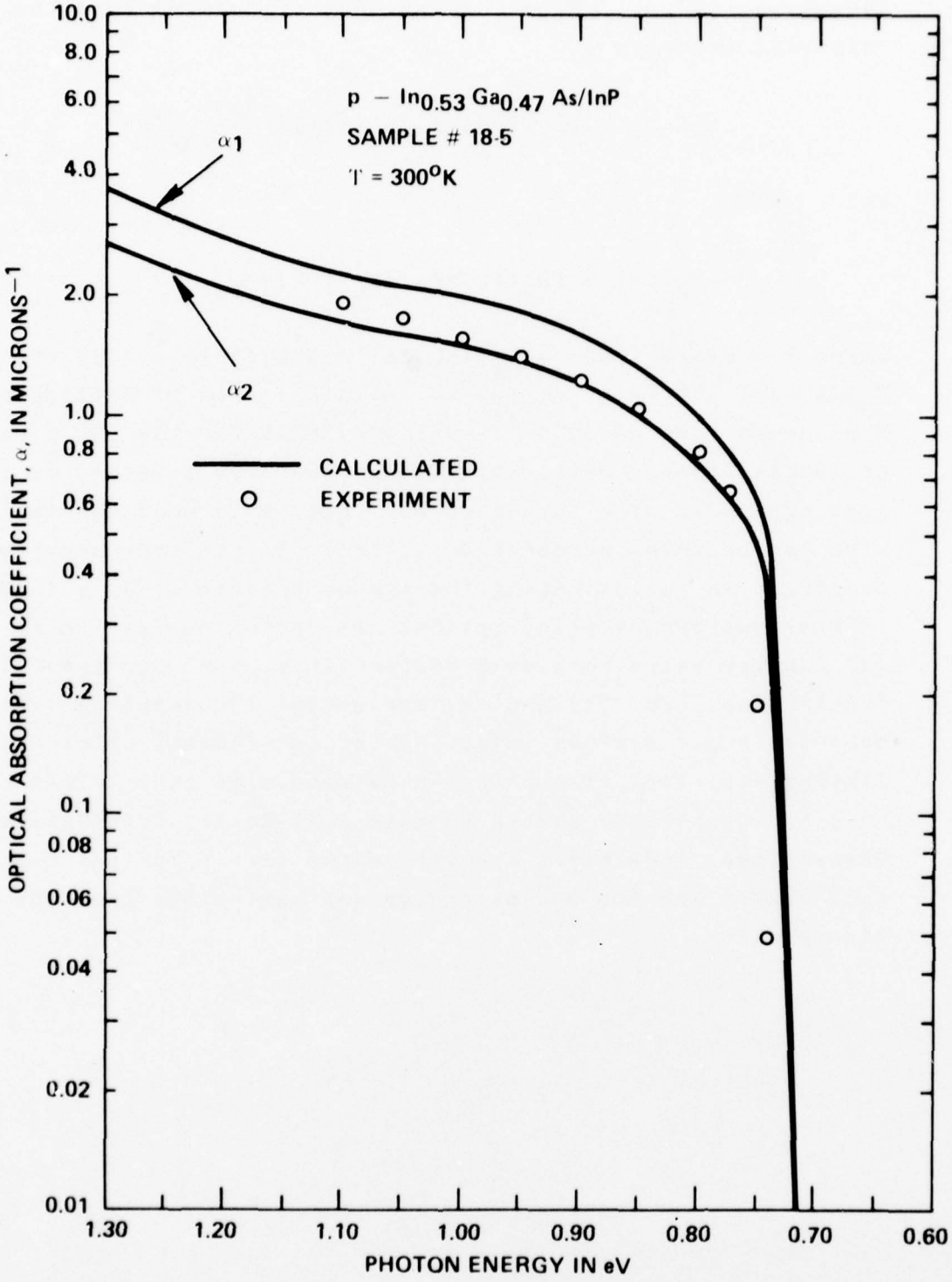

Fig. 7. Optical absorption coefficient versus photon energy for $In_{.53}Ga_{.47}As$.

curves, a_1 and α_2. These curves were calculated from the empirical formulas

$$\alpha_1(h\nu) = [E_g(InGaAs)/E_g(InP)]^{1/2}\alpha_{InP}(Y) \qquad (3)$$

and

$$\alpha_2(h\nu) = [E_g(InGaAs)/E_g(InP)]\alpha_{InP}(Y) \qquad (4)$$

where $Y \equiv h\nu + E_g(InP) - E_g(InGaAs)$ and $E_g(InP) = 1.35$ eV, $E_g(InGaAs) = 0.75$ eV at 300^oK. $\alpha_{InP}(h\nu)$ data of Philipp and Ehrenreich were used.[13,14] Using 0.75 eV for the 300^oK bandgap of InGaAs gives a reasonable fit to the α vs $h\nu$ data, is in good agreement with Takeda et al[12] and is in good agreement with our photoluminescence data. Eq. (3) has been used successfully in approximating the higher bandgap (1.35 - 1.10 eV) InGaAsP quaternary alloy optical absorption coefficients. Eq. (4) however seems to give a better fit to the experimental InGaAs data. Eq. (3) and (4) are useful for modeling various optoelectronic devices involving the InP-InGaAsP alloy system. Similar empirical relations can be used with other III-V ternary and quaternary alloys such as GaAs-GaAsP, GaAs-GaAlAs, GaAs-GaInAs, InP-InAsP, etc within the direct optical transition region and for modest energy gap variations from the binary alloy.

4. PHOTOLUMINESCENCE MEASUREMENTS ON $In_{.53}Ga_{.47}As/InP(100)$

Photoluminescence (PL) measurements have been routinely done on both n and p-type $In_{.53}Ga_{.47}As/InP$ samples. The bulk of these measurements were made at 77°K although occasionally 300°K data are taken. The PL setup consists of a Lexel Model 95-2, 2-W argon ion laser operating at 5145 Å (2.41 eV), a Perkin-Elmer Model 210 monochromator with 1.4 micron grating (640 lines/mm), and a PbS photoconductor detector (300°K). The laser beam is chopped at 82 Hz and the PL signal synchronously detected with a PAR Model HR8 lock-in amplifier. A dry-ice-cooled RCA Model 7102 photomultiplier (S-1) is used for higher energy PL measurements above about 1.0 eV. 77°K measurements are conveniently made by immersing the sample directly into a LN_2 dewar. This technique is relatively fast and allows a number of samples to be tested in a short time. The disadvantage is a certain amount of "bubble noise" due to the slow boil-off of the liquid.

Fig. 8 is a ≅ 300°K PL spectrum of an undoped, n-type $In_{.53}Ga_{.47}As/InP(100)$ sample #FB-PTO-629-19 with $n \cong 2 \times 10^{16}/cm^3$. When the radiative recombination is a band-impurity transition (i.e., valence band to shallow donor level), the photon energy PL peak is given by $h\nu(\text{PL peak}) = E_g - E_i + 1/2\ K_BT$, where E_g is the energy bandgap, E_i the impurity (donor) level, K_B the Boltzman constant, and T the temperature. The sample was not well heat sunk for the 300°K experiment and therefore the PL spectrum peak in Fig. 8 may be somewhat low due to sample heating effects. Takeda et al found the room temperature PL peak for n-type $In_{.53}Ga_{.47}As$ to be at 0.749 eV, 10 meV higher than our data. The full width at half maximum, FWHM, of the PL spectrum at 300°K is 55 meV in our case compared with 39 meV reported by Takeda et al.

Fig 9 shows the 77°K PL data for the same sample as that in Fig. 8. The PL signal strength is enhanced about a factor

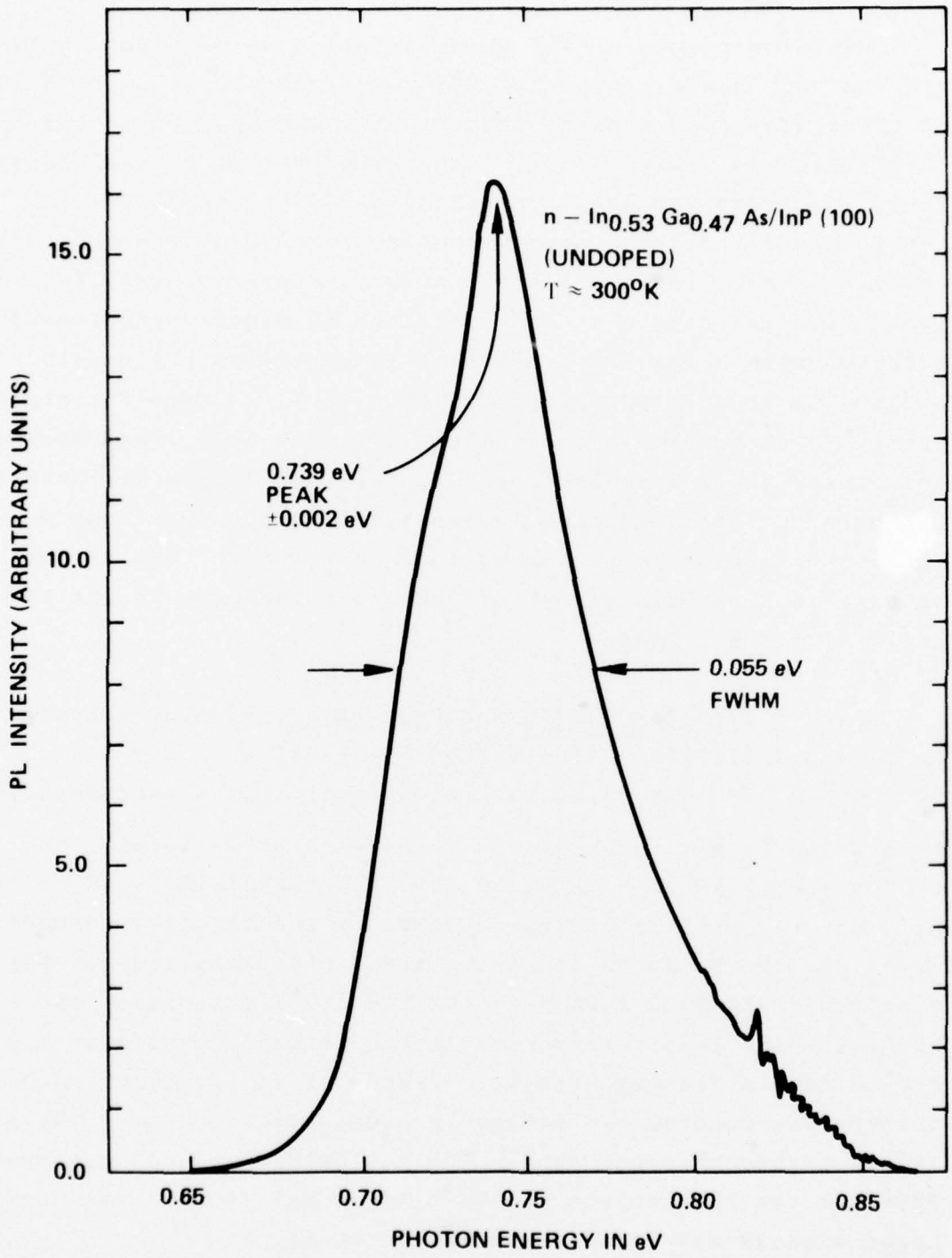

Fig. 8. Photoluminescence spectrum at 300°K from an undoped $In_{.53}Ga_{.47}As$ sample.

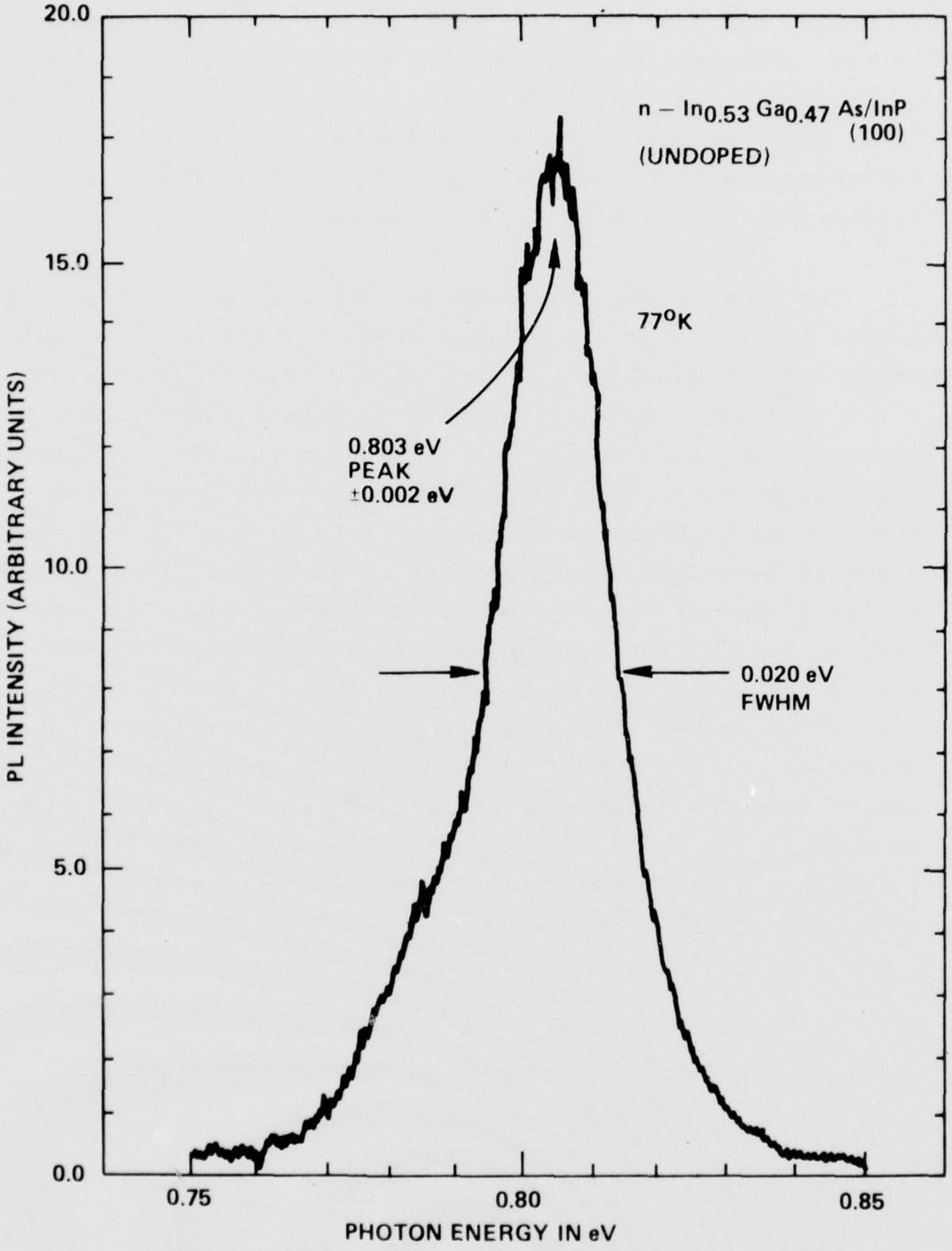

Fig. 9. Photoluminescence s[illegible] at 77°K from the same sample as that in [illegible].

of ≅ 50X, the peak moves to 0.803 eV and the FWHM decreases to 20 meV. Takeda's PL measurements showed a peak at 0.810 ev with a FWHM of 14 meV. This time there is a 7 meV difference in PL peak energies with our data again the lower energy. The difference could be due to simple calibration errors or slight composition differences between samples.

The bulk of the photocathode work has been with Zn-doped, p-type InGaAs. Fig. 10 shows a 77°K PL spectrum on sample #FA-PT-3901-0 which is Zn-doped with a hole concentration of $\simeq 5 \times 10^{16}/cm^3$. The main PL peak is within experimental uncertainty at the same energy as the undoped PL peak and represents transitions very close to band-to-band. The lower energy shoulder at 0.788 eV is associated with the Zn and represents conduction band to acceptor level transitions. From this we deduce $E_i(Zn)$ as 13 meV ± 4 meV in InGaAs. Also note that the FWHM is now 28 meV, 8 meV higher than the undoped PL spectrum due to the broadening effect of the Zn. As the Zn concentration is increased, the relative intensity of the Zn PL peak increases as well. Fig. 11 shows the 77°K PL spectrum from a higher Zn-doped sample, #FA-PT-5101-0, where the hole concentration is $\simeq 1 \times 10^{17}/cm^3$. In this case only the Zn peak is resolved. A similar behavior with Zn-doping is observed with InP where $E_i(Zn) \simeq 35$ meV.

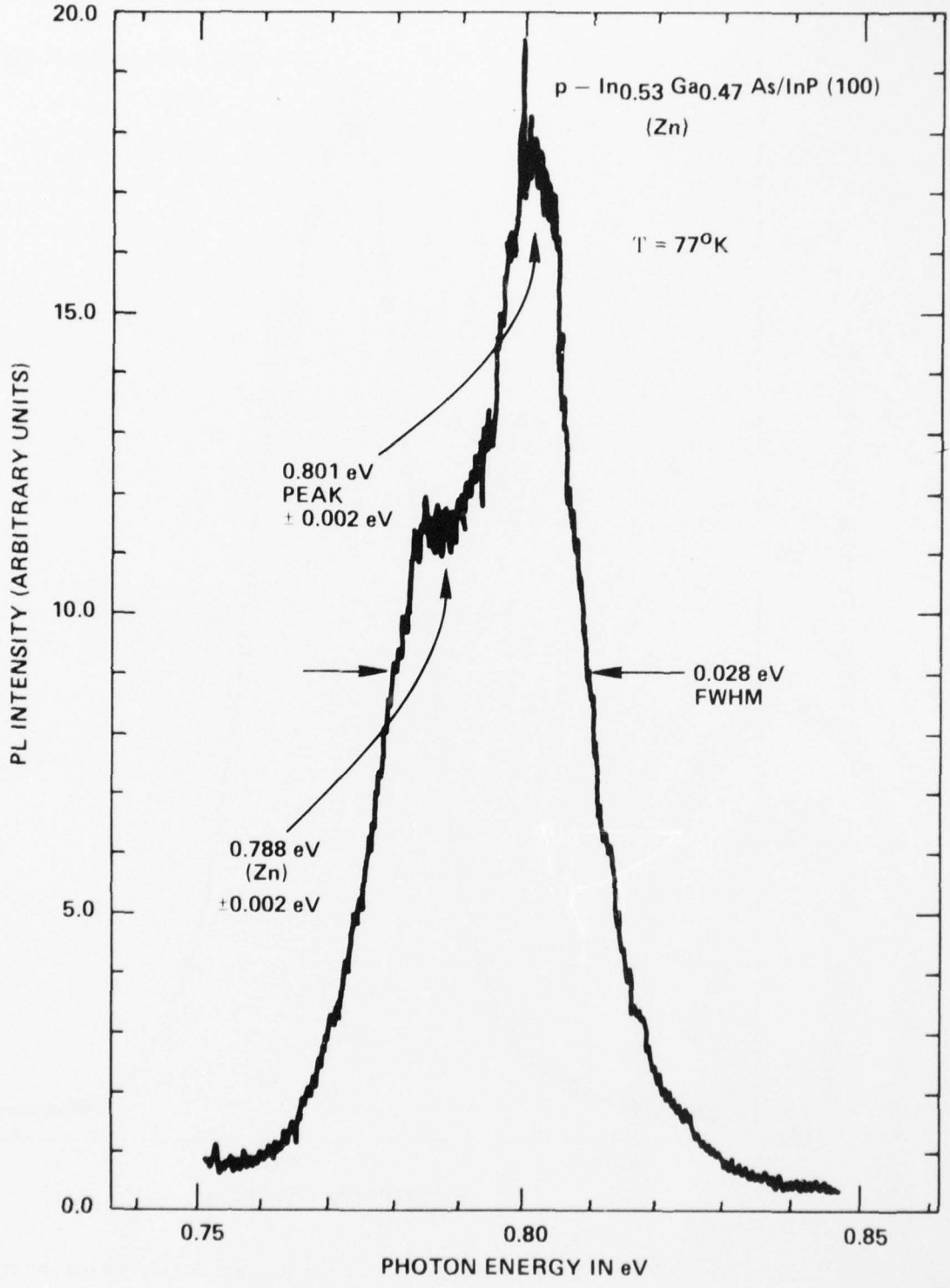

Fig. 10. Photoluminescence spectrum at 77°K from a low p-type $In_{.53}Ga_{.47}As$ sample.

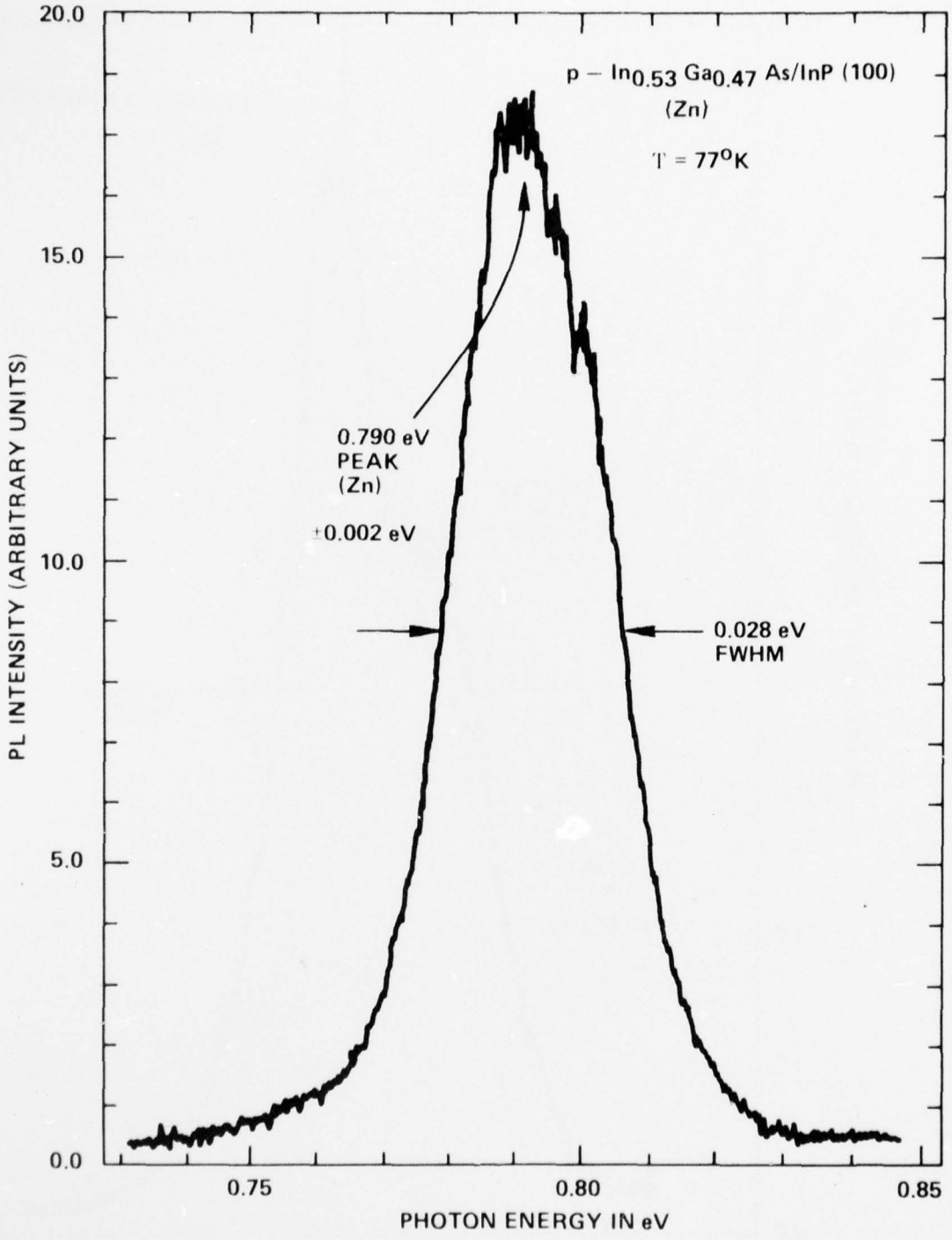

Fig. 11. Photoluminescence spectrum at 77°K from a higher p-type $In_{.53}Ga_{.47}As$ sample.

5. MONTE CARLO SIMULATION STUDIES OF THE TE PHOTOCATHODE

Work was begun in the fall of 1977 on a computer simulation of the electron transport processes in the field-assisted photocathode using the Monte Carlo technique. This work, performed by Dr. T.J. Maloney of this laboratory, has focused for the most part on the Ag/p-InP field-assisted cathode since most of our experimental work has been with this material and there is sufficient data on the necessary materials parameters needed for the program. Preliminary results of the InP calculations have been presented already[15,16] and plans are to publish a detailed account in the near future.

Monte Carlo methods have been successfully used in the past to simulate electron transport in semiconductors.[17] The technique has mostly been used to derive fundamental transport properties (e.g., average electron velocity, electron temperature, electron energy distributions) under constant-field conditions. The basic concept in such a computer simulation is to follow an electron, assumed to be typical, for a long time (or many electrons for a short time) in the solid, allowing it to be accelerated by the electric field, scattered by impurities and by the various phonons, transferred among the conduction valleys, and so on. Random numbers are used to select the time of flight between scattering events, the scattering process for a particular event, and the final state of the electron after the event, so that the behavior of a typical electron is simulated. By averaging the appropriate quantities over the total flight time one can derive such things as average velocity, energy and k-space histograms, electron temperature, and the startup transient (velocity vs time or distance) of electrons in a suddenly-applied field.

Although most Monte Carlo work on electron transport has been for simple constant-field conditions, it is in principle possible to use the technique to simulate a real electronic

device complete with nonuniform fields and even, if necessary, time dependence. Such efforts are likely to be frustrating and expensive if the device is, say, a field effect transistor with time dependent electric fields influenced by internal space charge.[18] However, the field-assisted photocathode lends itself particularly well to Monte Carlo simulation because time dependence is negligible and because the electron charge densities (set up by low light levels) are too low to influence the linearly graded electric field produced by the reverse bias on the Schottky-barrier. In the Monte Carlo model for the photocathode, electrons are generated in the bulk with a spatial distribution appropriate to the optical absorption coefficient for the chosen photon energy. The latter also determines the initial energy of the electron. When the electrons reach the semiconductor surface, the program takes note of the electron's energy, k-vector, and conduction band, then records this information before generating another electron in the bulk. The Monte Carlo simulation produces a profile of the elelctrons reaching the surface that helps predict the performance of a photocathode.

The emphasis in the calculations has been on studying the effects of applied bias and emitter doping on the energy distribution of photogenerated electrons. In the case of Ag/p-InP emitters, the Γ electrons tend to bunch up close to the bottom of the L valley at the emitting surface. See Fig. 12. This is a general feature of the calculations. For higher biases or higher doping, the number of Γ electrons decreases relative to those which transfer into the L and X valleys, as expected. See Fig. 13 and 14. The average energy in each valley also increases with bias and doping as can be seen in Fig. 15 and 16. Assuming a 0.77-eV Schottky-barrier height for Ag/p-InP[8], a work function of $\simeq$ 1.10 eV, and a doping level of $3 \times 10^{16}/cm^3$ fixes the vacuum level at the emitting surface 0.30 eV above the Γ valley, 0.01 eV below the L, and 0.21 eV below the X. Therefore there is an effective NEA condition for the

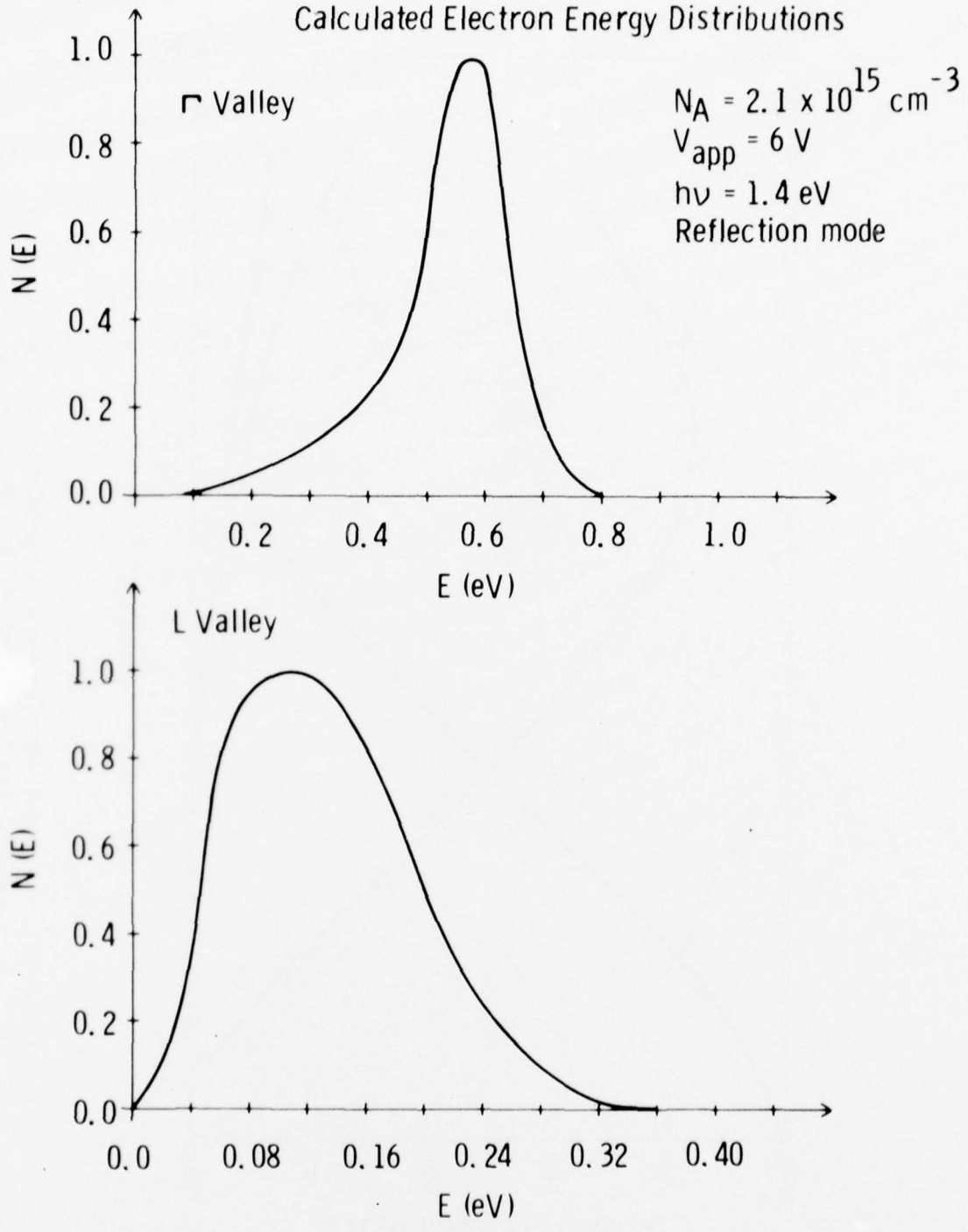

Fig. 12. Calculated electron energy distributions for a Ag/p-InP TE cathode. The zero of energy is taken to be the bottom of the Γ and L valley at the surface respectively. Note the difference in energy scales also.

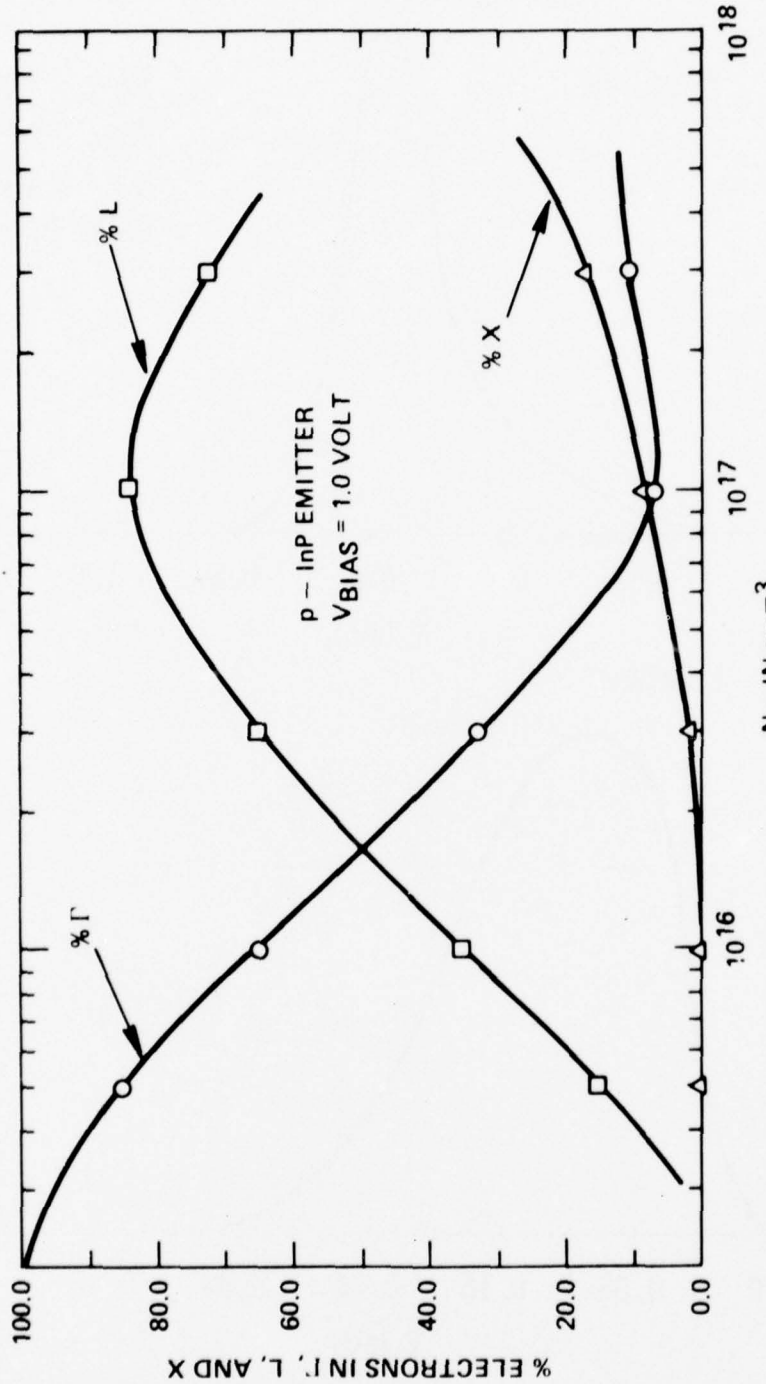

Fig. 13. Calculated electron energy population in the upper mass valleys versus p-type doping for a 1.0-V bias.

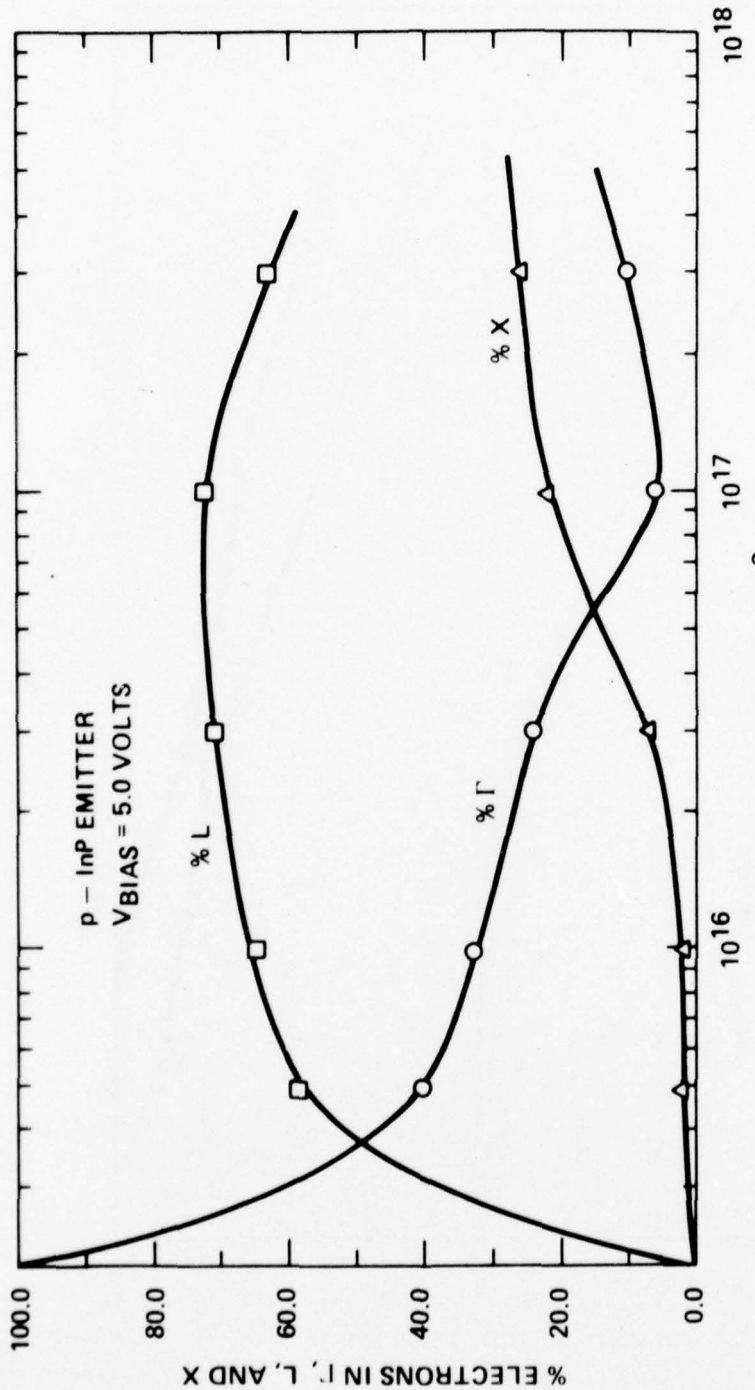

Fig. 14. Calculated electron energy population in the upper mass valleys versus p-type doping for a 5.0-V bias.

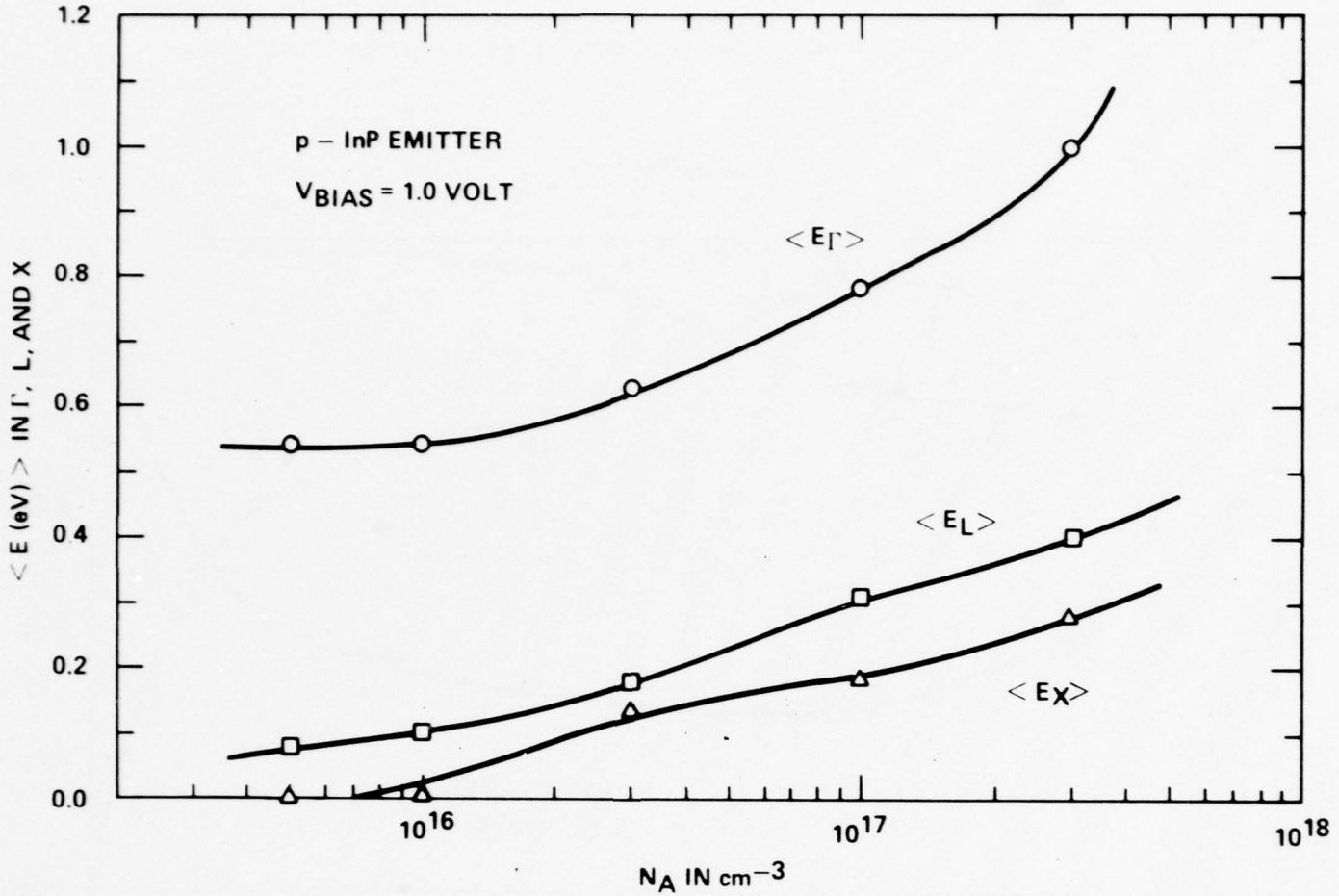

Fig. 15. Calculated mean electron energy in the upper mass valleys versus p-type doping for a 1.0-V bias.

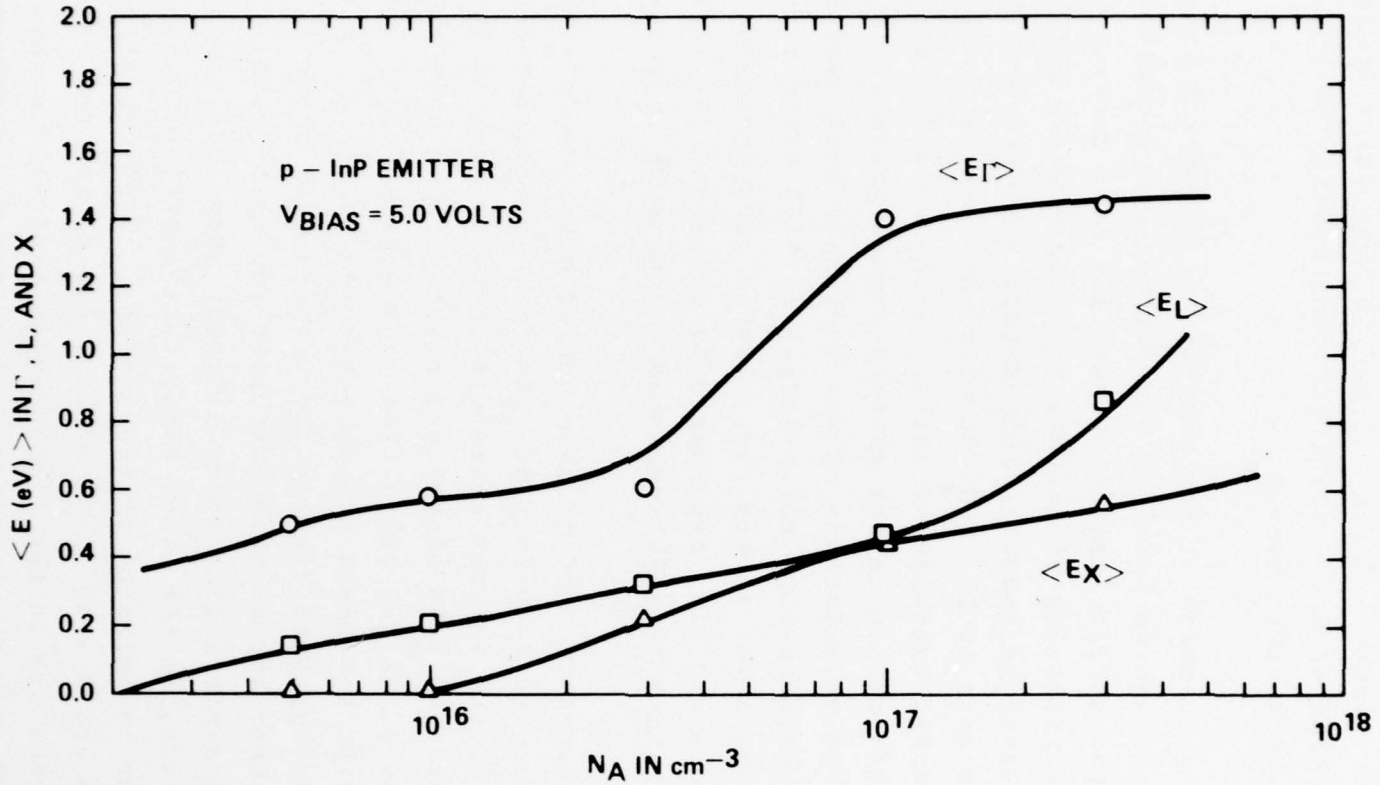

Fig. 16. Calculated mean electron energy in the upper mass valleys versus p-type doping for a 5.0-V bias.

higher mass valleys in the case of Ag/InP. It is also clear from the results of Fig. 15 and 16 that there could also be a fair number of hot Γ electrons contributing to the total electron current into vacuum.

The question of how many of the electrons whose energy is above the vacuum level at the surface can escape into vacuum, i.e., the surface escape probability is a difficult theoretical problem involving the matching of Bloch waves in the solid to plane waves in vacuum. Fortunately some research has been done in this area by Dr. M.G. Burt at the University of Cambridge.[20] In a recent exchange of letters with Dr. Burt, we have acquired some information on the surface escape probability from (111) InP. The calculations of Dr. Burt have been convolved with the Monte Carlo results for a Ag/p-InP(111)B cathode and compared with experiment in Fig. 17. Rather good agreement in both magnitude and bias dependence is achieved. Extension of these calculations to (100)-oriented emitters is under way.

Toward the end of this period Monte Carlo simulations have begun on the Ag/p-$In_{.53}Ga_{.47}As$ field-assisted cathode. Estimates of the various materials input parameters into the model were deduced from binary end point data on GaAs and InAs where necessary. A Γ-L conduction band separation of 0.85 eV was used with a 0.50-eV Schottky-barrier height.[19] A zero applied bias energy band diagram for this case is shown in Fig. 18. It is interesting to note that even for this cathode, the L valley at the surface lies at or slightly above the vacuum level. Γ electrons, on the other hand, face a 0.85-eV vacuum level barrier to emission at the surface. For a relatively high 5.0 V bias and 1 x $10^{15}/cm^3$ doping, 60% of the photogenerated electrons lie in the Γ conduction band with an average energy of 0.75 eV. The remainder are in the L conduction band with an average energy of 0.20 eV. For the same 5.0 V bias but 1 x $10^{16}/cm^3$ doping, only 37% are in the Γ conduction band with an average energy of 1.77 eV and the remainder in the L with an

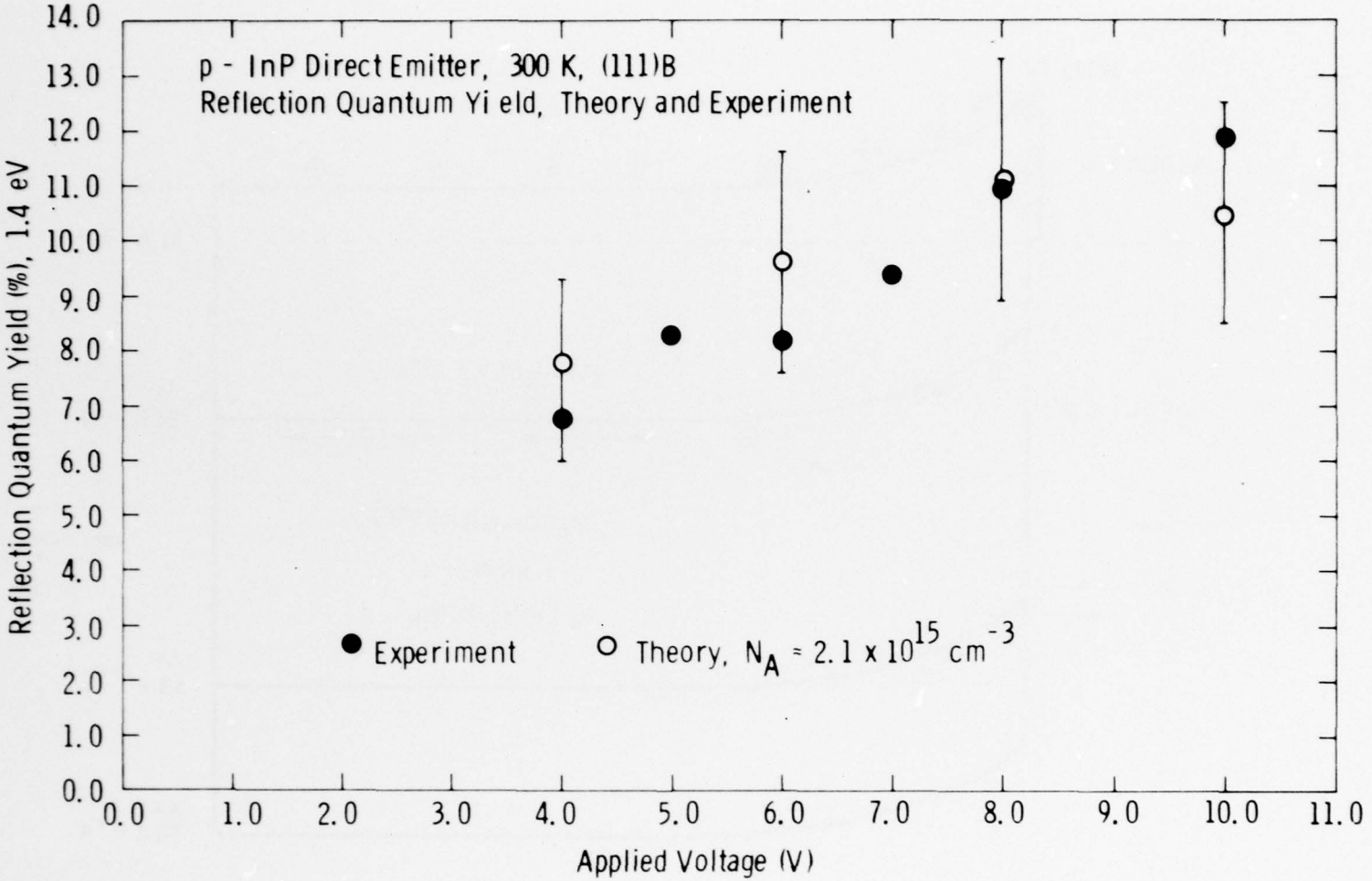

Fig. 17. Calculated and measured reflection-mode quantum yield versus applied bias for a Ag/p-InP TE cathode.

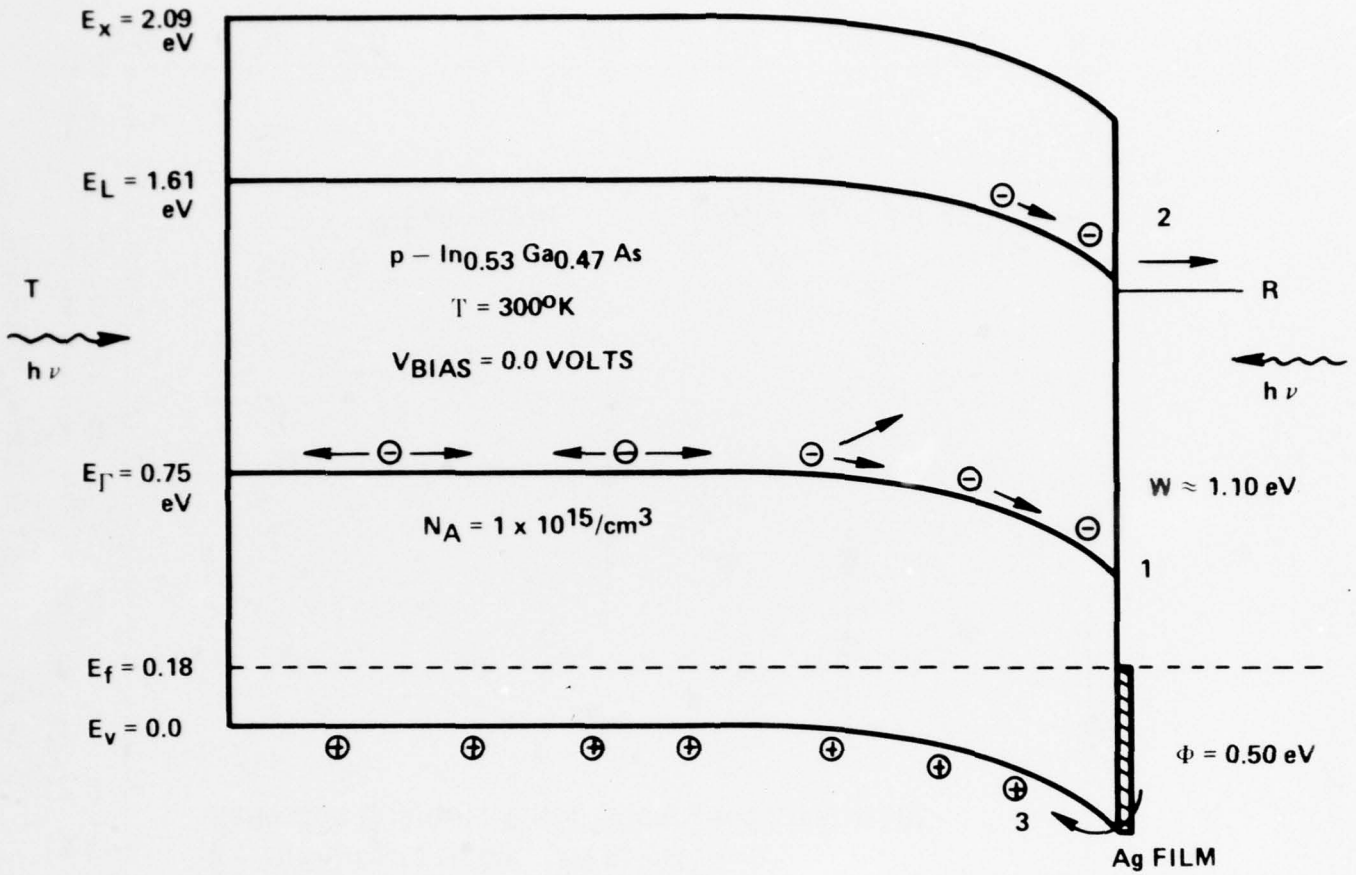

Fig. 18. Energy band diagram for a Ag/p-$In_{.53}Ga_{.47}As$ TE cathode under zero bas conditions:

average energy of 0.77 eV. Hence ignoring possible quantum mechanical surface escape probability effects, transferred electrons into the L conduction band and 0.85 eV or hotter Γ electrons will have a reasonable chance of being emitted into vacuum. Since the direct bandgap of $In_{.53}Ga_{.47}As$ is only 0.75 eV at $300^{o}K$, there is the possibility that the electrons will begin to avalanche even at low to modest bias voltages. This process was not included in the Monte Carlo calculations.

6. PHOTOEMISSION STUDIES OF Ag/p-$In_{.53}Ga_{.47}As$/InP PHOTOCATHODES

Vacuum processing of Ag/p-$In_{.53}Ga_{.47}As$ cathodes is identical to that used for Ag/p-InP emitters. Details of this process have been discussed elsewhere.[21] The first attempt at activating a Ag/InGaAs cathode was quite successful. See Fig. 19. At room temperature the Ag/p-InGaAs Schottky-barrier leakage in the reverse bias direction is often quite leaky due to the relatively low Schottky-barrier height on p-InGaAs of 0.5 eV. Cooling to about -100°C however is more than sufficient to reduce the internal Schottky-barrier junction current to permit several volts of reverse bias to be applied. As further materials improvements have been made or vacuum processing techniques optimized, other Ag/InGaAs cathodes have been vacuum tested. The main results of these experiments have recently been published.[22]

Within the last few months a record field-assisted yield of 1.6% at 1.3 microns from a Ag/p-InGaAs cathode was achieved. See Fig. 20. The cathode is LPE grown on a InP(100) substrate. The p-type dopant is Zn and the acceptor concentration is about $3 \times 10^{16}/cm^3$. The mobility is 100 cm^2/V-sec at 300°K. Interestingly this cathode failed to show any field-assisted photoemission at 300°K. The temperature dependence of the field-assisted yield is quite variable from sample to sample and the reason for its behavior is not certain at this time. Fig. 21 shows detailed photoemission yield data from a Ag/p-InGaAs cathode near threshold for three different cathode temperatures. The shift in threshold with temperature is due to the bandgap variation with temperature and is consistent with PL measurements discussed in Section 4.

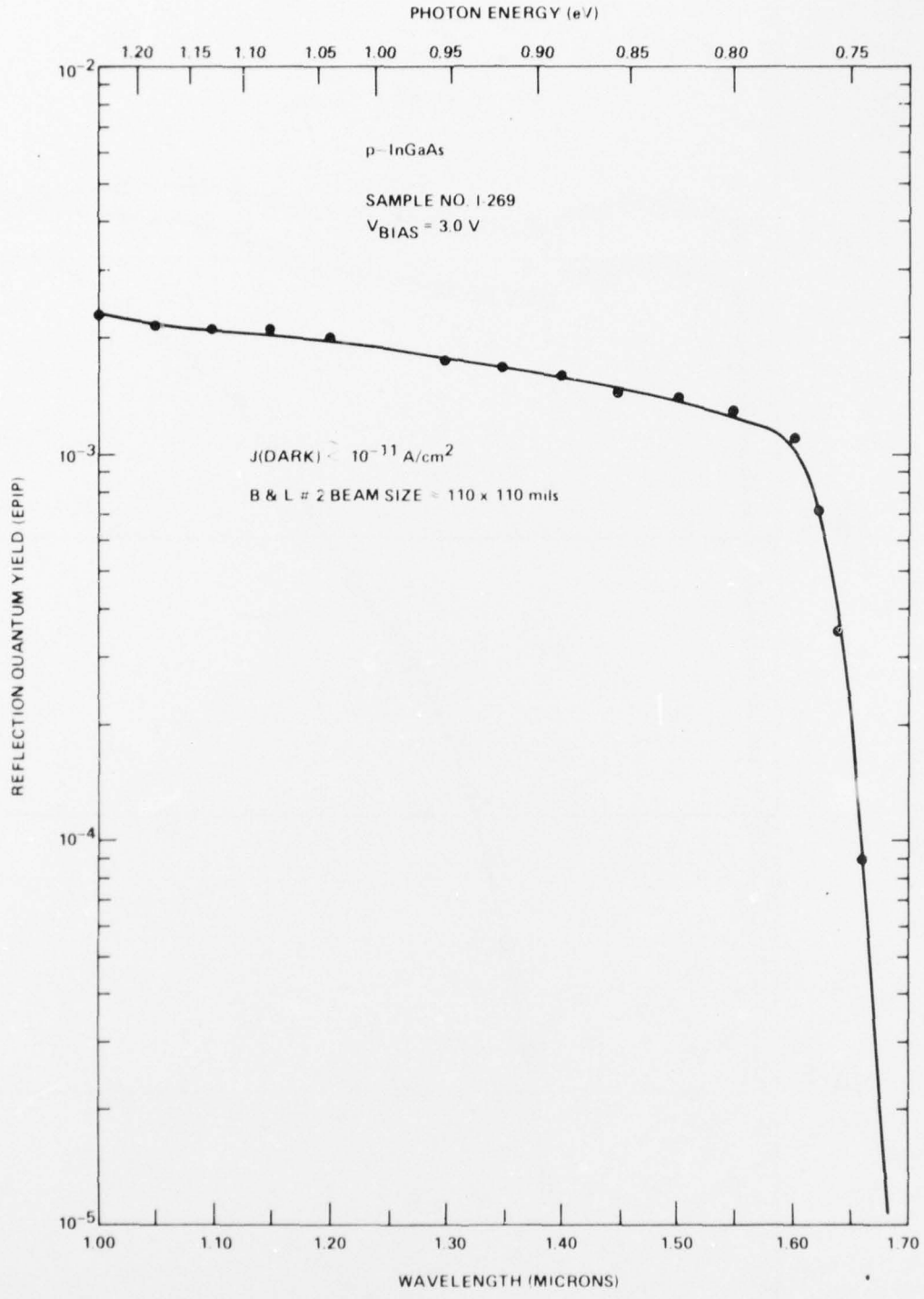

Fig. 19. Experimental reflection-mode quantum yield curve from a Ag/p-$In_{.53}Ga_{.47}As$ TE cathode.

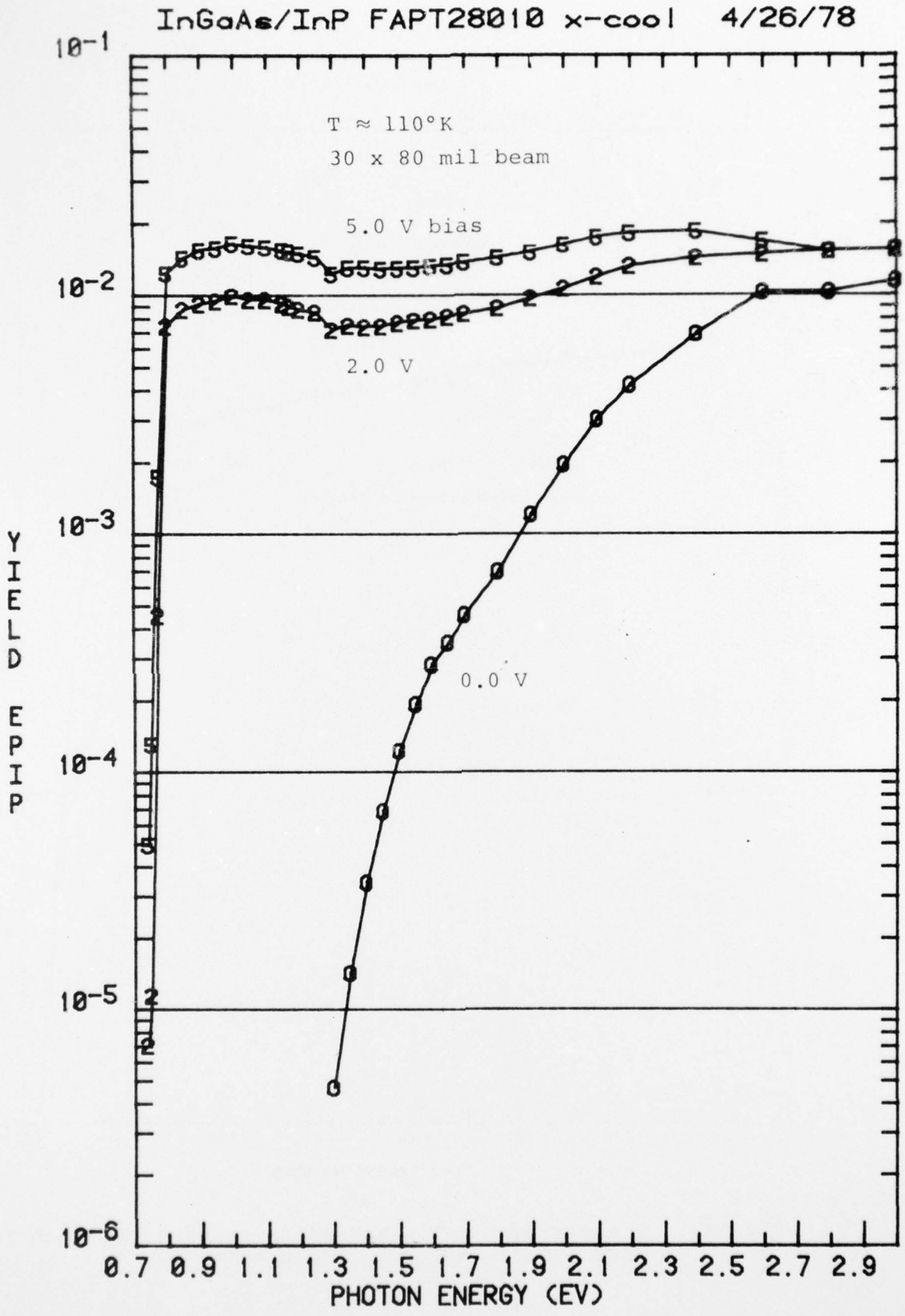

Fig. 20. Record experimental reflection-mode quantum yield achieved to date from a Ag/p-$In_{.53}Ga_{.47}As$ TE cathode.

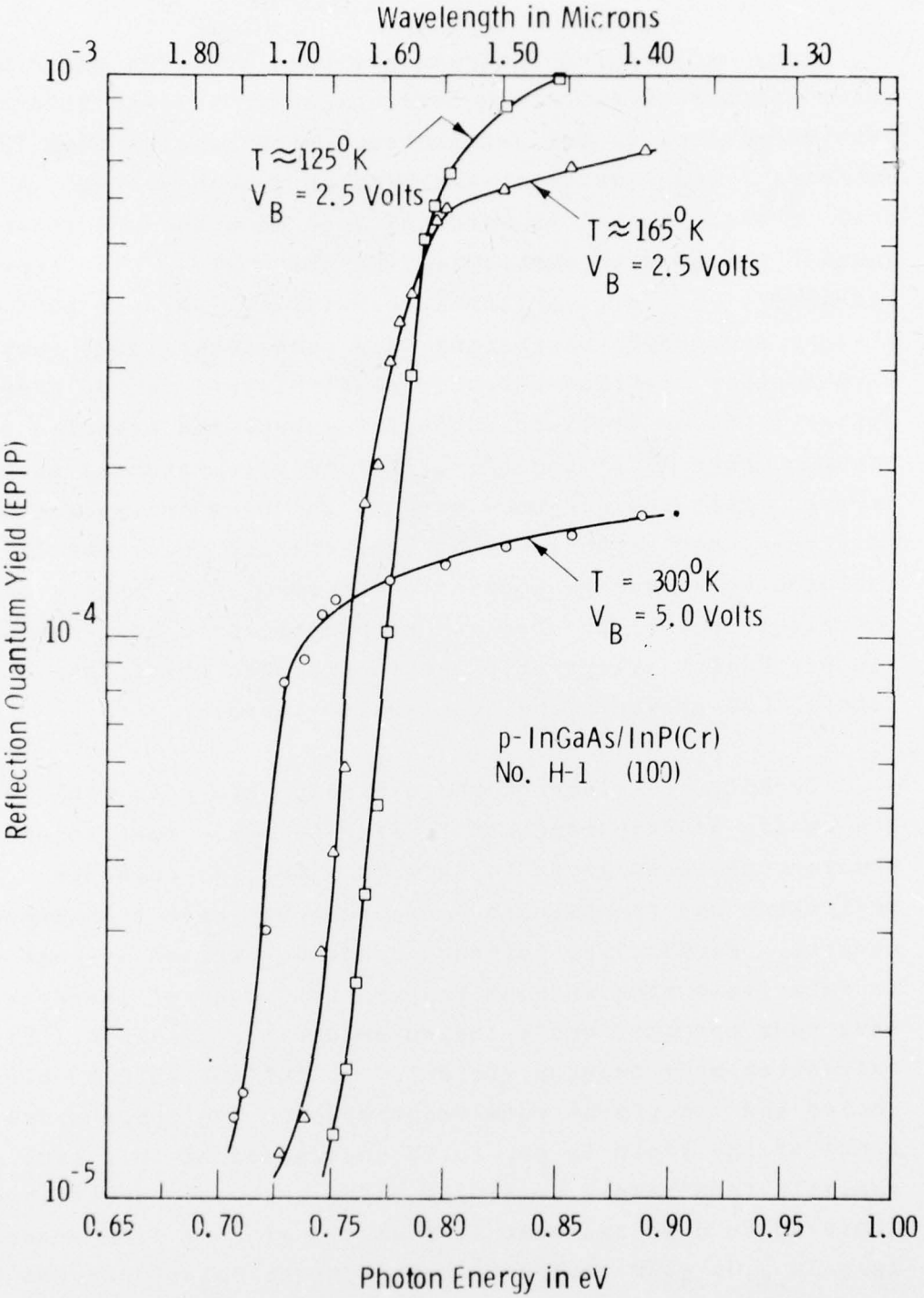

Fig. 21. Experimental reflection-mode quantum yield near threshold from a Ag/p-$In_{.53}Ga_{.47}As$ Te cathode for 300, 165, and 125°K operation.

7. CONCLUSIONS AND RECOMMENDATIONS

Very encouraging progress has been achieved under this contract in both materials development of InGaAsP alloys lattice-matched to InP and photoemission results from TE photocathodes in an experimental ultrahigh vacuum system. A great deal of basic materials work has gone into the LPE growth of InGaAsP alloys with particular attention given the lower bandgap alloys and $In_{.53}Ga_{.47}As$ in particular. Proper melt compositions and growth parameters have been established such that high quality, lattice-matched InGaAsP layers can be grown on either (100) or (111)-oriented InP substrates over the entire bandgap range (1.35 to 0.75 eV) of lattice-matching quaternaries. Photoluminescence and Van der Pauw analysis techniques have been used extensively to characterize the grown layers in addition to vacuum photoemission activations. Sharp, strong photoluminescence spectra and high mobilities are characteristic of InGaAsP alloys when lattice-matched conditions and careful LPE-growth techniques are followed.

Transferred-electron photoemission has been achieved over the entire bandgap range of InGaAsP alloys. Most attention, however, has been given to Ag/p-$In_{.53}Ga_{.47}As$ cathodes. Both reflection and transmission-mode response have been demonstrated. Because the internal Schottky-barrier leakage current is relatively high at room temperature, most of these cathodes have been operated under cooled conditions, ~ 150°K. Typical reflection-mode quantum yield is ~ 0.10% out to 1.65 microns cooled and ~ 0.01% at room temperature. The temperature dependence of the yield is not fully understood at this time and is variable from sample to sample. The best quantum efficiency achieved to date has been 1.6% at 1.3 microns from a cooled Ag/p-$In_{.53}Ga_{.47}As$ cathode. Dark current emission seems to be associated with an impact ionization mechanism from hot holes from the internal Schottky-barrier junction current.

A number of areas of investigation can be cited for further research. In the materials area there is more work needed in further improving the quality of growth of $In_{.53}Ga_{.47}As$ alloys both in terms of electrical properties and cosmetics. Of particular interest would be the study of impurity and alloy scattering mechanisms in relation to electron and hole mobilities in InGaAsP alloys. Also there is a need to study deep levels in this material since such levels could possibly play an important role in both the temperature dependence of the photoemission and the dark current emission from InGaAsP alloy TE cathodes. Although reasonably good success has been achieved with the InGaAsP alloys in terms of photoemission results, there has been very little work done on other III-V systems that could potentially offer higher quantum efficiency, longer wavelength response, room temperature operation, or lower dark current emission.

In the vacuum photoemission area there are a number of areas in which further work is warranted. There is more work needed on understanding the physics of electron emission from TE cathodes. One useful technique is electron energy distribution measurements. These measurements, although difficult to perform experimentally, should offer valuable information on the emission process. These measurements could conveniently be compared with the Monte Carlo simulation model programmed for the TE cathode. More work is needed on optimizing the vacuum activation procedures used to process TE cathodes and a great deal more work is needed on understanding dark current emission. The mechanism of dark current emission needs to be firmly established as well as viable techniques to minimize dark current emission. Detailed internal junction and dark current versus bias and temperature measurements would be helpful.

In summary it can be said that the TE cathode has already demonstrated outstanding potential as a 1-2 micron photocathode. However, there is clearly much more investigative work to be done before the full potential and limitations of this device are known.

8. REFERENCES

1. R.L. Bell, L.W. James, and R.L. Moon, Appl. Phys. Lett. 25, 645 (1974).

2. W. Fawcett and D.C. Herbert, J. Phys. C 7, 1641 (1974).

3. R.E. Hayes and R.M. Raymond, Appl. Phys. Lett. 31, 300 (1977).

4. R.L. Bell, Negative Electron Affinity Devices (Clarendon Press, Oxford, 1973).

5. J.S. Escher and R. Sankaran, Appl. Phys. Lett. 29, 87 (1976).

6. I.P. Molodyan, S.I. Radautsan, E.V. Russu, and S.V. Slobodchikov, Sov. Phys. Semicond. 8, 879 (1975).

7. R. Sankaran, R.L. Moon, and G.A. Antypas, J. Crystal Growth 33, 271 (1976).

8. R. Sankaran, G.A. Antypas, R.L. Moon, J.S. Escher, and L.W. James, J. Vac. Sci. Technol. 13, 932 (1976).

9. S.B. Hyder, G.A. Antypas, J.S. Escher, and P.E. Gregory, Appl. Phys. Lett. 551 (1977).

10. G.A. Antypas and L.Y. Shen, Inst. Phys. Conf. Er. No. 33b, 96 (1977).

11. G.A. Antypas, Y.M. Houng, S.B. Hyder, J.S. Escher, and P.E. Gregory, Appl. Phys. Lett, 33, 463 (1978).

12. Y. Takeda, A. Sasaki, Y. Imamura, and T. Takagi, J. Appl. Phys. 47, 5405 (1976).

13. H.R. Philipp and H. Ehrenreich, Phys. Rev. 129, 1550 (1963).

14. B.O. Seraphin and H.E. Bennett in Semiconductors and Semimetals, eds. R.K. Willardson and A.C. Beer (Academic Press, N.Y. 1967), Vol. 3, Chap. 12.

15. J.S. Escher, T.J. Maloney, P.E. Gregory, S.B. Hyder, and Y.M. Houng, "Photoemission to 1.7 Microns from a InP/InGaAs Transferred-Electron Photocathode," paper presented at the 1978 Device Research Conference, UC Santa Barbara, June 1978. Also an informal talk given by T.J. Maloney entitled "Electron Transport in Field-Assisted Photoemitters," presented at the Workshop on Hot-Electron Phenomena in Semi-conductors, Cornell University, Ithaca, N.Y., August 1978.

16. Semi-Annual Technical Report No. 7 under Contract DAAK02-74-C-0132 and Progress Reports for January 1 through June 30, 1978 and July 1 through December 31, 1977 under this contract.

17. T.J. Maloney and J. Frey, J. Appl. Phys. 48, 781 (1977) and references therein.

18. R.W. Hockney et al, Electron. Lett. 10, 484 (1974).

19. J.S. Escher, L.W. James, R. Sankaran, G.A. Antypas, R.L. Moon, and R.L. Bell, J. Vac. Sci. Technol. 13, 874 (1976).

20. M.G. Burt and J.C. Inkson, J. Phys. D 9, 43 (1976) and references therein.

21. See reports under Contract DAAK02-74-C-0132.

22. J.S. Escher, P.E. Gregory, S.B. Hyder, and R. Sankaran, J. Appl. Phys. 49, 2591 (1978).

9. LIST OF PUBLICATIONS

1. R.L. Bell, L.W. James, and R.L. Moon, Appl. Phys. Lett. 25, 645 (1974).

2. J.S. Escher, R.D. Fairman, G.A. Antypas, R. Sankaran, L.W. James, and R.L. Bell, CRC Rev. in Solid State Sciences 5, 577 (1975).

3. J.S. Escher and R. Sankaran, Appl. Phys. Lett. 29, 87 (1976).

4. R. Sankaran and G.A. Antypas, J. Crystal Growth 36, 198 (1976).

5. J.S. Escher, L.W. James, R. Sankaran, G.A. Antypas, R.L. Moon, and R.L. Bell, J. Vac. Sci. Technol. 13, 874 (1976).

6. S.B. Hyder, G.A. Antypas, J.S. Escher, and P.E. Gregory, Appl. Phys. Lett. 31, 551 (1977).

7. J.S. Escher, P.E. Gregory, G.A. Antypas, R. Sankaran, and Y.M. Houng, J. Appl. Phys. 49, 447 (1978).

8. J.S. Escher, P.E. Gregory, S.B. Hyder, and R. Sankaran, J. Appl. Phys. 49, 2591 (1978).

9. P.E. Gregory, J.S. Escher, S.B. Hyder, Y.M. Houng, and G.A. Antypas, J. Vac. Sci. Technol. (to be published July/August 1978).

10. G.A. Antypas, Y.M. Houng, S.B. Hyder, J.S. Escher, and P.E. Gregory, Appl. Phys. Lett. (to be published Sept. 1978).